

1 **Response to Anonymous Referee #1**

2
3 Comment: This study represents a credible attempt at a new way to infer surface PM_{2.5} levels
4 from CALIOP data, on a regional, two-year average basis. An advantage of CALIOP over passive
5 sensors for this sort of analysis is the fact that it measures vertical profiles of backscatter and
6 depolarisation, so bypasses a limitation inherent with imager data in partitioning between total
7 column and near-surface aerosol loadings. In contrast, an acknowledged limitation is the curtain
8 sampling of CALIOP vs. the broad-swath sampling of MODIS, etc. The authors introduce their
9 technique and explain the relevant assumptions, and show results over the USA, evaluated with
10 EPA monitors. This is a sensible, strong first step in this direction. The topic is important and
11 relevant to AMT. I have a number of comments (below) but on the whole recommend that the
12 paper can be accepted after minor revisions. Hopefully this will be a springboard for further studies
13 refining the technique and expanding to other regions and time periods.

14
15 Response: We thank the reviewer for his/her comments and encouragement.

16
17 Comment: As a general comment, much of the quantitative evaluation is presented as scatter plots
18 with linear regression fits, and the discussion is often framed in terms of r^2 and slope. I'm not sure
19 that this is the right thing to do here. One reason is that my understanding is that there can be non-
20 negligible uncertainties on the PM data. Indeed, Ayers (2001,
21 <https://www.sciencedirect.com/science/article/pii/S1352231000005276>) recommends using
22 reduced major axis (RMA) regression instead of ordinary least squares when comparing PM
23 monitors, for that reason. But also, the analysis in section 3 indicates that the CALIOP-derived
24 estimates seem to have PM-dependence on their uncertainties too, so standard RMA may not be
25 right either (as that assumes independent identically-distributed errors). For this reason I'd
26 recommend Deming regression as a reasonable alternative
27 (https://en.wikipedia.org/wiki/Deming_regression) when trying to compute the best-fit line. This
28 should be more appropriate for this case, has packages in standard programming languages (and
29 is not hard to code anyway), and is not hard to interpret. So this should be a pretty straightforward
30 change to make which would improve the rigor of the manuscript. I recommend this is done
31 throughout. Or, alternatively, don't fit a line but report something like mean ratio and RMS across
32 certain ranges by binning the data.

33 I think it is important that appropriate statistical methods be used; continued publication using
34 techniques we know to be deficient for our analyses just normalizes and encourages bad practice
35 in the future. There isn't really a good justification for not fixing this.

36 Response: Thank you for the comments and suggestions. As recommended, Deming regression
37 best-fit lines were added to the scatterplots of Figs. 1, 3, 4, 8, and 9, and the slopes computed from
38 the Deming regression analyses were added to Tables 2, 3, and 4. Corresponding changes in regard
39 to these figures and tables were made to the narrative, and the following was added to the end of
40 Section 2 to describe Deming regression: "Lastly, we note that most of the results are shown in the
41 form of scatter plots with fits from Deming regression (Deming, 1943). Due to uncertainties in
42 PM_{2.5} data, we show slopes computed from Deming regression analyses instead of those from
43 simple linear regression. Deming regression in particular is appropriate here, as it accounts for

44 errors in both the independent and dependent variables (Deming, 1943), and has been used in past
45 PM_{2.5} related studies (e.g., Huang et al., 2014).”

46 Comment: My remaining comments are given as PXX, LYYY referring to page and line numbers
47 respectively.

48 P1L21: I suggest replacing “sizes” with “diameters”, as that is my understanding of the definition,
49 but the remote sensing community often refers to radius instead when discussing size.

50 Response: Thank you for this suggestion. We have made the recommended changes.

51 Comment: P4L95: I am curious as to why, with over 10 years of data, the two-year period 2008-
52 2009 is used here? If sampling is a limiting factor in some areas, surely adding a few more years
53 would help with this? Is there something special about these two years, or some a priori reason
54 why two years provides sufficient sampling? I realize that running the whole mission is probably
55 not feasible at this stage. But I would imagine that in the time between this comment being posted
56 and the close of Open Discussion, there would be sufficient time to download and analyze an
57 additional few years of data. This should mostly be a matter of storage and CPU time, since the
58 code is already written (and since the first author is at Langley where CALIPSO is based, I doubt
59 computational concerns would be significant here).

60 Response: The two-year period of 2008-2009 was chosen because we wanted to be consistent with
61 the temporal domain of our previous PM_{2.5} study (Toth et al., 2014). An explanation is included
62 in Section 2. We agree that adding more years would increase sampling, but we feel this is more
63 appropriate for a future paper, as the purpose of this manuscript is to provide an initial
64 demonstration of the concept. An extended analysis is planned for a forthcoming paper.

65
66 Comment: P6L123: somewhere in this initial paragraph, I’d ideally like some more discussion of
67 the EPA data. For example, what are the uncertainties, is there any significant difference in these
68 between the TEOM and BAM methods, and is there a difference in the siting of these two
69 instrument types? If they’re super-accurate and precise and equivalent, that’s important to know.
70 But if one is better than the other, and there’s some spatial/temporal clustering in when TEOM vs.
71 BAM is employed, that is also important to know. Recently, Kiss et al (2017, [https://www.atmos-
72 meas-tech.net/10/2477/2017/](https://www.atmos-meas-tech.net/10/2477/2017/)) published an analysis showing biases in hourly PM10
73 measurements. Is that relevant here? It might be, especially since that some daily averages in the
74 EPA data correspond to a single sample. These are examples of things I’d like to see covered in
75 the opening part of this section.

76
77 Response: Thank you for the comment. As for the Kiss et al. (2017) study, PM data with a lower
78 temporal resolution (like 24-hour, “daily” data) are less biased compared to hourly data. Still,
79 uncertainties in hourly data are likely to impact daily data that are averaged from hourly data. To
80 fully quantify this issue would deserve a paper of its own. Here, as suggested by the reviewer, we
81 have edited the discussion in this section to incorporate uncertainties of the various PM_{2.5}
82 measurements and spatial representativeness of the different instruments/methods. The following
83 was added to the text:
84

85 “Note that uncertainties have been reported for hourly PM measurements (Kiss et al., 2017).
86 Examples of some uncertainties in these PM_{2.5} measurements depend upon the instrument/method
87 used: gravimetric (e.g., transport to the lab/human error and volatilization of PM during the drying
88 process; Patashnick et al., 2001), TEOM (e.g., errors due to improper inlet tube temperature;
89 Eatough et al., 2003), and beta attenuation monitors (e.g., changes in the sample flow rate due to
90 variations in temperature and moisture; Spagnolo, 1989). Also, it has been found that beta
91 attenuation monitors may be more accurate than TEOM, as TEOM can underestimate PM_{2.5} at low
92 temperatures (e.g., Chung et al., 2001). Still, as suggested by Kiss et al. (2017), PM data collected
93 over a longer period of time are much less likely to be biased. Thus, we expect lower uncertainties
94 from data collected over 24-hours, then daily data generated by averaging hourly observations.
95 Fully quantifying the differences from the two different PM observing methods, however, is a
96 subject for a future study.”

97 Comment: P8L189-190: This assumption (negligible mass above 10 micron size) is probably
98 reasonable. But it would be fairly easy to try and quantify with AERONET. Take the inversion
99 product from a half-dozen AERONET sites and count the fraction of the volume size distribution
100 above 10 microns (and note here that the AERONET retrievals report size in terms of radius, while
101 PM definitions are in diameter). You have to make some assumption about the density of particles
102 being the same across the size range, but otherwise that gives a first order estimate at how big the
103 effect might be, which could be compared to the other parts of the uncertainty analysis in section
104 3.2. I think AERONET dust radius peaks somewhere like 2.5 microns so in the western US, it
105 might be that there’s some dust contribution from the tail of the distribution which is being
106 systematically missed here and would lead to an overestimate in the CALIOP-derived PM levels.
107 Maybe it is negligible, but it would be fairly easy to show that it is negligible, and the authors have
108 not.

109 Response: It is a nice idea but we think it might be difficult to apply the proposed idea for the US
110 for a few reasons. Firstly, reliable AERONET volume size distributions are obtained from
111 inversions that are performed when the 440 nm AOD is larger than 0.4 (Dubovik et al., 2006). In
112 this study, we emphasize studying 2-year means over the US, which rarely exhibit averaged 440
113 nm AODs larger than 0.4. Secondly, we are only concerned with near surface (100-1000 m)
114 aerosols for this study, but AERONET would provide values for the entire column, making such
115 a comparison difficult. We argue that our assumption of negligible mass above 10 microns is
116 reasonable because dust has been excluded from the analysis, and sea salt represents a small
117 fraction of aerosols in the 100-1000 m atmospheric layer over the US for the 2008-2009 time
118 period (i.e., < 2%). Thus, we did not implement this change as suggested.

119 Comment: P13L299: An alternative to this (whether for the sensitivity analysis or the analysis as
120 a whole) might be to look at the whole boundary layer (determining on a case by case basis) rather
121 than testing different height ranges. Assuming that boundary layer depth is included as part of the
122 MERRA2 meteorology being used here? This would go from assuming “the surface level of PM
123 is represented well by the atmospheric layer from 0.1-1 km” to assuming “the boundary layer is
124 well-mixed so represents the surface PM well”, which is subtly different and might work better. I
125 do agree that it seems reasonable to exclude the lowest 100 m, though.

126 Response: Thank you for this suggestion. Unfortunately, boundary layer depth is not included in
127 the MERRA-2 meteorological profiles used for this analysis. MERRA-2 relative humidity was
128 chosen for the paper because it was already collocated with the CALIOP aerosol profiles. A
129 boundary layer depth analysis would not be a straightforward task, and we believe a thorough
130 study into this important topic is best left for another paper during which our method can be further
131 refined.

132
133 Comment: P14L323: This section made me wonder why the authors do not estimate PM10 from
134 CALIOP, and evaluate that, in addition to PM2.5? This would remove the need for an assumption
135 of the ratio (taken as 0.6 here), and line 326 notes that there are 409 EPA stations providing both
136 data on a daily basis. Given that this ratio seems to be one of the more uncertain parts of the error
137 budget, it might be that there is more skill in predicting PM10 from CALIOP. Or it might go the
138 other way. That would also be a worthwhile result, since right now we don't know.

139
140 Response: We did not estimate PM10 from CALIOP because coarse mode aerosols exhibit vastly
141 different mass extinction efficiency values than those of fine mode aerosols. We have included an
142 initial look into an analysis of coarse mode aerosols, like dust and sea salt, in Table 4, the results
143 of which suggest that large uncertainties would arise for CALIOP-derived PM values assuming
144 coarse mode aerosols as fine mode aerosols. In order to tackle this subject, a more thorough
145 investigation into CALIOP/ground-based aerosol typing is necessary, and we believe this topic is
146 outside the general scope of this paper.

147 Comment: P17L382: No particular comment here other than to say I am glad that the authors
148 included this specific analysis. It's a point well-made that CALIOP uncertainties propagate
149 downwards so, while CALIOP can see through thin clouds, that does not mean that the data quality
150 is the same as for cloud-free columns.

151 Response: Thank you for your thoughts on this topic.

152 Comment: P19L424: This isn't really an uncertainty analysis, so I suggest promoting it from a
153 section 3.2.9 to a section 3.3 by itself. I also have a few suggestions for expansion of this section.
154 It's good to know the correlation lengths across the western vs. eastern USA, but there's a lot of
155 scatter in the plots. Some of this is probably due to limited sampling but some is probably also due
156 to real changes in correlation length. So I wonder if the authors can pull out data from one or two
157 large cities, and one or two remote areas, and highlight the correlation lengths for these (as well as
158 the more general case of east vs. west). This would provide a bit more context about typical
159 correlation lengths in these conditions, which would be helpful for future research built around
160 this analysis.

161 Response: We agree that Section 3.2.9 is not an uncertainty analysis, and it has been changed to
162 Section 3.3. Concerning the other suggestions, each data point on the plot represents the distance
163 of the given two locations as well as the corresponding PM correlation computed using
164 observations from the two locations. Thus, the datasets are rather discrete and not continuous, as
165 the correlations can only be computed with any two locations with PM observations. Thus,
166 correlation lengths may not be derived reliably using only one or two cities. Still, we emphasize

167 here that this section is not the focus of the study, and can be explored in a more careful manner
168 in a later paper.

169

170 Papers cited:

171

172 Chung, A., Chang, D. P., Kleeman, M. J., Perry, K. D., Cahill, T. A., Dutcher, D., ... & Stroud, K:
173 Comparison of real-time instruments used to monitor airborne particulate matter, *Journal of the*
174 *Air & Waste Management Association*, 51(1), 109-120, 2001.

175

176 Deming, W.E.: *Statistical Adjustment of Data*, Wiley: New York, 1943.

177 Dubovik, O., Sinyuk, A., Lapyonok, T., Holben, B. N., Mishchenko, M., Yang, P., Eck, T. F.,
178 Volten, H., Muñoz, O., and Veihelmann, B.: Application of spheroid models to account for aerosol
179 particle nonsphericity in remote sensing of desert dust, *J. Geophys. Res.–Atmos.*, 111,
180 <https://doi.org/10.1029/2005JD006619>, 2006.

181 Eatough, D. J., Long, R. W., Modey, W. K., and Eatough, N. L.: Semi-volatile secondary organic
182 aerosol in urban atmospheres: meeting a measurement challenge, *Atmospheric*
183 *Environment*, 37(9-10), 1277-1292, 2003.

184

185

186 Huang, X. H., Bian, Q., Ng, W. M., Louie, P. K., and Yu, J. Z.: Characterization of PM_{2.5} major
187 components and source investigation in suburban Hong Kong: a one year monitoring
188 study, *Aerosol Air Qual. Res.*, 14(1), 237-250, 2014.

189

190 Kiss, G., Imre, K., Molnár, Á., and Gelencsér, A.: Bias caused by water adsorption in hourly PM
191 measurements, *Atmos. Meas. Tech.*, 10, 2477-2484, <https://doi.org/10.5194/amt-10-2477-2017>,
192 2017.

193

194

195 Patashnick, H., Rupprecht, G., Ambs, J. L., and Meyer, M. B.: Development of a reference
196 standard for particulate matter mass in ambient air, *Aerosol Science & Technology*, 34(1), 42-45,
197 2001.

198

199 Spagnolo, G. S.: Automatic instrument for aerosol samples using the beta-particle attenuation,
200 *Journal of aerosol science*, 20(1), 19-27, 1989.

201

202 Toth, T. D., Zhang, J., Campbell, J. R., Hyer, E. J., Reid, J. S., Shi, Y., and Westphal, D. L.: Impact
203 of data quality and surface-to-column representativeness on the PM_{2.5} / satellite AOD relationship
204 for the contiguous United States, *Atmos. Chem. Phys.*, 14, 6049-6062,
205 <https://doi.org/10.5194/acp-14-6049-2014>, 2014.

206

207

208

209 **Response to Anonymous Referee #2**

210 Comment: The scope of the submitted work is to investigate the potential exploitation of CALIOP
211 extinction profiles in order to derive near-surface concentrations of particles with aerodynamic
212 diameter less than 2.5 μm (PM_{2.5}). The assessment of the applied methodology is made through
213 the evaluation of the CALIOP derived PM concentrations against corresponding daily ground-
214 based measurements obtained at numerous EPA stations, over the period 2008-2009, distributed
215 across CONUS, which is the area of interest. A powerful element of using vertically resolved
216 retrievals is that the altitude range can be constrained (i.e., near surface where the PM
217 concentrations are measured from the ground) in contrast to passive sensors which are
218 representative for the whole atmospheric column. To my opinion, the issues addressed by the
219 authors fit well to the scientific objectives of AMT and therefore I recommend the submitted
220 manuscript to be published. Nevertheless, I believe that several points must be modified making
221 the text acceptable for publication. My major and minor comments are listed below.

222 Response: Thank you for your thoughts and encouraging comments.

223 Comment: The authors have used only 2-year satellite data thus making the robustness of the
224 obtained outcomes questionable taking into account CALIOP's low sampling frequency and
225 narrow footprint. In order to overcome this drawback, you have to repeat the analysis for the full
226 dataset.

227 Response: We agree that overcoming this sampling drawback can be achieved through extending
228 the analysis for more than two years. However, this would be computationally expensive and is a
229 non-trivial task. We envisioned this manuscript as a proof-of-concept study, the purpose of which
230 is to provide an initial demonstration of the feasibility of our method. Adding other years to the
231 analysis will be one of the focuses of forthcoming CALIOP/PM_{2.5} papers.

232 Comment: According to the applied methodology, all the aerosol extinctions assigned as dust in
233 the CALIOP retrieval algorithm are masked out since focus is given on the small size particles
234 (Lines 198-200). However, which is the treatment for the other aerosol subtypes consisting of
235 coarse particles (i.e., marine, dusty marine)? Moreover, what is happening when the aerosol
236 subtype is clean continental? I would suggest to repeat the aerosol type analysis (Section 3.2.8)
237 but considering only the CALIOP aerosol subtypes which are not associated with large size
238 particles (i.e., dust, marine, marine dust) and are relevant to pollution. Keep in mind that
239 appropriate modifications, depending on aerosol types, may be needed in equations 1, 2 and 3 (i.e.,
240 mass scattering and absorption efficiencies, hygroscopic growth factor).

241 Response: All aerosol subtypes not classified as dust are considered for our method (e.g., marine,
242 dusty marine, clean continental, etc.). We have already excluded dust, and most areas of the
243 CONUS are not dominated by sea salt aerosols. Indeed, a statistical analysis showed that CALIOP
244 100-1000 m aerosol layers consisting entirely of marine (dusty marine) subtypes represent only
245 ~2% (~1%) of all subtypes. Thus, the impact of including these aerosols should be minor. We do
246 note, however, that one of the areas of focus for future studies of CALIOP-derived estimates is a
247 more thorough investigation into aerosol typing.

248 Comment: Could you please comment why the quality assurance criteria applied here are different
249 than those suggested by Tacket et al. (2018; <https://www.atmos-meas-tech.net/11/4129/2018/>)?

250 Response: The QA criteria applied for this paper are the same as those of our previous CALIOP
251 papers (e.g., Toth et al. 2014; 2016; 2018), and we wanted to be consistent with these studies. The
252 QA scheme employed here was developed from Kittaka et al. (2011) and Campbell et al. (2012),
253 both of which provide detailed justifications for the QA choices made. Toth et al. (2016) provides
254 comparisons of aerosol extinction profiles using our QA scheme and those from the CALIPSO
255 Level 3 aerosol profile product. While some differences were found, these were mostly attributed
256 to differences in averaging, treatment of clouds and fill values, and our vertical regridding from
257 60 m to 100 m.

258 Comment: Page 7 – Lines 157-160: The inclusion of different PM measurements techniques (filter-
259 based or averages from hourly samples) how can affect the intercomparison results?
260

261
262 Response: As suggested by Kiss et al. (2017), large uncertainties exist in hourly PM data, while
263 less biases are expected for PM data collected over a longer period of time. Thus, there are likely
264 differences in the two methods for collecting PM data. Still, to fully explore this issue requires a
265 study of its own, and thus we have added the following discussions in the text:
266

267 “Note that uncertainties have been reported for hourly PM measurements (Kiss et al., 2017).
268 Examples of some uncertainties in these PM_{2.5} measurements depend upon the instrument/method
269 used: gravimetric (e.g., transport to the lab/human error and volatilization of PM during the drying
270 process; Patashnick et al., 2001), TEOM (e.g., errors due to improper inlet tube temperature;
271 Eatough et al., 2003), and beta attenuation monitors (e.g., changes in the sample flow rate due to
272 variations in temperature and moisture; Spagnolo, 1989). Also, it has been found that beta
273 attenuation monitors may be more accurate than TEOM, as TEOM can underestimate PM_{2.5} at low
274 temperatures (e.g., Chung et al., 2001). Still, as suggested by Kiss et al. (2017), PM data collected
275 over a longer period of time are much less likely to be biased. Thus, we expect lower uncertainties
276 from data collected over 24-hours, then daily data generated by averaging hourly observations.
277 Fully quantifying the differences from the two different PM observing methods, however, is the
278 subject for a future study.”

279 Comment: Page 4 – Lines 97-102: How much reliable are the scatterplot metrics when MODIS
280 provides daylight AODs while PM concentrations are daily averages? Have you noticed any
281 variation both in spatial and temporal terms?

282 Response: In this paper, we have not looked into the spatial/temporal variations of MODIS AOD
283 versus PM_{2.5}. This, however, was the subject of one of our past studies (Toth et al., 2014), for
284 which MODIS AOD was compared to both daily (within 1x1 deg.) and hourly (within 40 km)
285 PM_{2.5} measurements. While larger correlation coefficients were found for the hourly analysis,
286 they still remained low. The purpose of Fig. 1 in this paper was to simply illustrate the limitation
287 of using column-integrated AOD from passive sensors to estimate PM_{2.5} concentrations near the
288 surface.
289

290 Comment: Page 9 – Line 202: A couple of citations are needed here in order to support this
291 argument.

292
293 Response: We have added two citations (Nessler et al., 2005 and Lynch et al., 2016), as requested.
294

295 Comment: Page 10 – Lines 236-238: It will be useful to provide a map with the number of days
296 participating for the calculation of the average maps illustrated in Figure 3. Moreover, it is required
297 a geographical distribution providing the average number of profiles considered for the derivation
298 of 1° x 1° grid cells (i.e. an indicator of spatial representativeness within the 1deg grid cell).

299 Response: Thank you for this suggestion. We have added the requested maps as a figure in an
300 appendix. Also, the following description was added to the text in Section 3.1: “Note that, for
301 context, maps of the number of days and CALIOP Level 2 5 km aerosol profiles used in the
302 creation of Fig. 3a-d are shown in Appendix Fig. 1.”

303 Comment: Page 12 – Lines 270-279: I don’t agree with the collocation criteria applied here. The
304 horizontal distance (100 km) between CALIOP and PM station probably is too long since the
305 analysis focuses on PM_{2.5} originating from pollution. Under these cases it is expected that the
306 horizontal variability will be very strong and the concentrations will decrease rapidly for increasing
307 distance from the source. As it concerns the temporal collocation, the optimum solution would be
308 to use PM measurements available at the finest temporal resolution thus making feasible an
309 appropriate matching with the CALIOP near-surface profiles. On the contrary, if the ground-based
310 data are provided only as daily averages then you cannot consider that a satellite overpass and a
311 daily average are temporally collocated. In the former data you have an instantaneous observation
312 while in the latter one the diurnal variation is included. In case where the EPA data are given only
313 on a daily basis, then it is more convenient to compare “daily” CALIOP profiles (considering dates
314 where both the daytime and nighttime satellite retrievals are available) against the corresponding
315 surface PM₁₀ concentrations. For this reason, I believe that Figures 3-e and 3-f as well as the
316 relevant parts of the text must be removed. Please consider this comment throughout your analysis.

317 Response: Thanks for the suggestion. We agree that “daily” averaged CALIOP profiles may be
318 used for comparing with daily averaged surface PM observations. However, with a narrow swath
319 of ~70 m and a repeat cycle of 16 days, very few data points would be available within 100 km of
320 a particular EPA site for both daytime and nighttime CALIOP aerosol profiles. For the spatial
321 collocation, the +/- 100 km collocation distance is used here, as we considered the spread of
322 aerosols within 24 hours. For example, for a 10 km/hour wind speed, aerosol particles may travel
323 200 km (or +/- 100 km) within 24 hours. Also, as suggested from this paper, the averaged e-
324 folding correlation length for PM_{2.5} concentrations over the CONUS is ~600 km, and thus we
325 believe 100 km is a reasonable collocation range.
326

327 Also, analysis using finer temporal resolution PM_{2.5} data may produce better results under some
328 conditions, but comes with its own issues. For example, there are insufficient collocated CALIOP
329 profiles and hourly PM_{2.5} data over a two-year period for the CONUS, so the temporal domain
330 would need to be greatly expanded. Secondly, this type of study would take careful analysis of
331 the CALIOP data, as individual CALIOP aerosol extinction profiles could be subject to higher

332 uncertainties (e.g., rather than using a two-year mean). These research topics will be examined in
333 detail in future studies.

334 Comment: Section 3.2.1: Considering my previous comment, the analysis should be presented
335 only for the “daily” CALIOP – PM pairs and not separately for daytime and nighttime. Likewise,
336 the CALIOP derived PM_{2.5} ranges (x axis in Figure 5) should be equally sampled and not grouped
337 based on user-defined bins of PM concentrations. In addition, the authors are stating in Lines 314-
338 316 that the computations have not been done for PM concentrations $\geq 25 \mu\text{g m}^{-3}$ due to the limited
339 number of concurrent annual means. However, according to Figure 5, the number of samples for
340 the lowest bin ($< 5 \mu\text{g m}^{-3}$) during daytime is almost zero (the same is valid for the highest bins,
341 particularly for the nighttime retrievals). Is that correct? Can we trust the calculated RMSEs
342 resulting from a very small number of samples?

343 Response: As mentioned in another response, using only “daily” CALIOP-PM pairs is not feasible
344 here for a robust analysis, due to the repeat cycle of the CALIPSO satellite. Very few data points
345 would be available within 100 km of a particular EPA site for both daytime and nighttime CALIOP
346 aerosol profiles. Thus, we leave daytime and nighttime separated for this figure. As for the
347 CALIOP derived PM_{2.5} ranges, we have adjusted them such that each bin is equally sampled
348 based upon a cumulative histogram analysis. Each point from left to right in the new Fig. 5
349 represents the RMSE and mean PM_{2.5} concentration derived from CALIOP for 0-20%, 20-40%,
350 40-60%, 60-80%, and 80-100% cumulative frequencies. This addresses the other items in this
351 comment, like those of few samples for the lowest and highest bins in the old Fig. 5. Because they
352 are now equally sampled, we have removed the secondary y-axis since the number of samples do
353 not change as a function of CALIOP-derived PM_{2.5} concentration. We have also revised the
354 corresponding text in Section 3.2.1 as follows: “As a first step for the uncertainty analysis, we
355 estimated the prognostic error of 2-year averaged PM_{2.5,CALIOP}. Figure 5 shows the root-mean-
356 square error (RMSE) of CALIOP-based PM_{2.5} concentrations against those from EPA stations as
357 a function of CALIOP-based PM_{2.5} for the 2008-2009 period over the CONUS. RMSEs were
358 computed for five equally sampled bins, determined from a cumulative histogram analysis. Each
359 point in Fig. 5, from left to right, represents the RMSE and mean PM_{2.5} concentration derived from
360 CALIOP for 0-20%, 20-40%, 40-60%, 60-80%, and 80-100% cumulative frequencies. A mean
361 combined daytime and nighttime RMSE of $\sim 4 \mu\text{g m}^{-3}$ is found, with a mean value slightly greater
362 for nighttime ($\sim 4.3 \mu\text{g m}^{-3}$) than daytime ($\sim 3.7 \mu\text{g m}^{-3}$). While most bins exhibit larger nighttime
363 RMSEs, daytime RMSEs are larger for the greatest mean CALIOP-derived PM_{2.5} concentrations.”

364 Comment: Section 3.2.2: To my opinion this sensitivity study should be the first step of the analysis
365 in order to define the most “representative” altitude range. According to the summary statistics
366 presented in Table 2, it seems that it is better to restrict the upper bound at 600 – 700m.

367 Response: While a surface layer up to about 600-700 m results in larger r^2 values, much variability
368 in the statistics exists between surface layer heights (as shown in Table 2). Also, differences are
369 found between daytime and nighttime for various layers. One possible issue is a lower signal-to-
370 noise ratio if we restricted the surface layer to lower heights. We stress that the purpose of this
371 paper is an initial exploration of the topic, and wanted to include Table 2 as a first look at surface
372 layer height sensitivity. Another study is necessary to better evaluate this subject, especially as
373 surface layer height changes regionally and diurnally.

374 Comment: Section 3.2.4: Which is the impact on the r^2 values?

375 Response: The r^2 values are not impacted by varying the PM_{2.5}/PM₁₀ ratio. This is because all
376 of the CALIOP-derived PM_{2.5} points for each scenario shown in Table 3 are multiplied by a
377 common ratio (see Equation 3), but the collocated EPA concentrations remain unchanged (thus
378 not altering the correlation).

379
380 Comment: Section 3.2.5: Instead of presenting daytime and nighttime CALIOP derived PM
381 concentrations it is better to consider only the daily (computed from the concurrent daytime and
382 nighttime profiles) ones (see comment 6).

383 Response: Thank you for the suggestion. We believe it is important to show the daytime and
384 nighttime analyses separately, and an analysis using concurrent daytime and nighttime profiles
385 collocated with a particular EPA site will not yield many samples due to the repeat cycle of the
386 CALIPSO satellite. Thus we didn't make the change.

387 Comment: Page 19 – Lines 448-450: This means that the CALIOP derived PM concentrations are
388 not reliable in coastal (contamination by sea-salt particles) or dust affected regions?

389 Response: The large uncertainties are because mass extinction efficiencies are drastically different
390 for coarse and fine mode aerosols. Here we applied mass extinction efficiencies from fine mode
391 aerosols to coarse mode aerosols, and not surprisingly, see large uncertainties. Lower uncertainties
392 can be expected if we apply coarse mode mass extinction efficiencies to coarse mode aerosols.
393 However, this puts the pressure on accurate estimations of aerosol types from CALIOP or other
394 lidar observations, which we believe is a study of its own, and will be investigated in future studies.

395 Comment: Section 3.2.9: In this section it would be also useful to provide a map with the distances
396 where the $1/e$ value is found at each station.

397 Response: Thank you for this suggestion. However, for each pair of PM observing locations, one
398 correlation value is computed for a given distance between the two locations. Thus, the analysis
399 is discrete, not continuous. The $1/e$ values are estimated from Fig. 10, which is composed of
400 individual points representing both a distance and spatial PM_{2.5} correlation between pairs of EPA
401 sites over the CONUS. If we apply the same analysis to a given PM observing location, it is likely
402 to have data gaps due to the discrete nature of the dataset. Thus, we leave Fig. 10 untouched.

403 Comment: Page 3 – Lines 81-84: Could you please explain better this sentence?

404 Response: We have rewritten the sentence to:

405
406 “Indeed, Kaku et al. (2018) recently showed that surface PM_{2.5} had longer spatial correlation
407 lengths than AOD, even in the “well behaved” southeastern United States where previous studies
408 showed good correlation between PM_{2.5} and AOD (e.g., Wang and Christopher, 2003).”

409
410

411 Comment: Page 4 – Lines 91-94: It is not clear what the authors want to say here.

412 Response: We have rewritten the sentence to:

413

414 “It is arguable that from a climatological/long-term average perspective, the use of AOD as a
415 proxy for PM_{2.5} concentrations nevertheless has certain qualitative skill (e.g., Toth et al., 2014;
416 Reid et al., 2017) due to the averaging process that suppresses sporadic aerosol events with highly
417 variable vertical distributions.”

418 Comment: Page 10 – Line 244: What do you mean exactly here? (“..., as surface layer heights may
419 change seasonally and diurnally.”)

420 Response: We have removed “as surface layer heights may change seasonally and diurnally” to
421 avoid confusion.

422 Comment: Page 19 – Line 431: Sulfate & organic or just sulfate?

423 Response: To avoid confusion, we removed “& organic”. But primary and secondary biogenic
424 aerosols are mostly fine mode as well.

425 Comment: Page 20 – Lines 456-458: Please rephrase this sentence.

426 Response: This sentence was broken into two sentences, as follows: “To accomplish this, all EPA
427 stations over the CONUS with at least 50 days of daily data available for the 2008-2009 period
428 were first determined. Next, the distances between each pair of these EPA stations, and their
429 corresponding correlation of daily PM_{2.5} concentrations, were computed.”

430

431

432 Papers cited:

433

434 Campbell, J. R., Tackett, J. L., Reid, J. S., Zhang, J., Curtis, C. A., Hyer, E. J., Sessions, W. R.,
435 Westphal, D. L., Prospero, J. M., Welton, E. J., Omar, A. H., Vaughan, M. A., and Winker, D. M.:
436 Evaluating nighttime CALIOP 0.532 μm aerosol optical depth and extinction coefficient retrievals,
437 Atmos. Meas. Tech., 5, 2143-2160, <https://doi.org/10.5194/amt-5-2143-2012>, 2012.

438

439 Chung, A., Chang, D. P., Kleeman, M. J., Perry, K. D., Cahill, T. A., Dutcher, D., ... & Stroud, K:
440 Comparison of real-time instruments used to monitor airborne particulate matter, Journal of the
441 Air & Waste Management Association, 51(1), 109-120, 2001.

442

443 Deming, W.E.: Statistical Adjustment of Data, Wiley: New York, 1943.

444 Eatough, D. J., Long, R. W., Modey, W. K., and Eatough, N. L.: Semi-volatile secondary organic
445 aerosol in urban atmospheres: meeting a measurement challenge, Atmospheric
446 Environment, 37(9-10), 1277-1292, 2003.

447

448
449 Huang, X. H., Bian, Q., Ng, W. M., Louie, P. K., and Yu, J. Z.: Characterization of PM_{2.5} major
450 components and source investigation in suburban Hong Kong: a one year monitoring
451 study, *Aerosol Air Qual. Res.*, 14(1), 237-250, 2014.
452
453 Kiss, G., Imre, K., Molnár, Á., and Gelencsér, A.: Bias caused by water adsorption in hourly PM
454 measurements, *Atmos. Meas. Tech.*, 10, 2477-2484, <https://doi.org/10.5194/amt-10-2477-2017>,
455 2017.
456
457 Kittaka, C., Winker, D. M., Vaughan, M. A., Omar, A., & Remer, L. A.: Intercomparison of
458 column aerosol optical depths from CALIPSO and MODIS-Aqua, *Atmospheric Measurement*
459 *Techniques*, 4(2), 131, <https://doi.org/10.5194/amt-4-131-2011>, 2011.
460
461 Lynch P., and coauthors: An 11-year global gridded aerosol optical thickness reanalysis (v1.0) for
462 atmospheric and climate sciences, *Geosci. Model Dev.*, 9, 1489-1522, doi:10.5194/gmd-9-1489-
463 2016, 2016.
464
465 Nessler, R., Weingartner, E., and Baltensperger, U. (2005). Effect of humidity on aerosol light
466 absorption and its implications for extinction and the single scattering albedo illustrated for a site
467 in the lower free troposphere, *Journal of Aerosol Science*, 36(8), 958-972.
468
469 Patashnick, H., Rupprecht, G., Ambs, J. L., and Meyer, M. B.: Development of a reference
470 standard for particulate matter mass in ambient air, *Aerosol Science & Technology*, 34(1), 42-45,
471 2001.
472
473 Spagnolo, G. S.: Automatic instrument for aerosol samples using the beta-particle attenuation,
474 *Journal of aerosol science*, 20(1), 19-27, 1989.
475
476 Toth, T. D., Campbell, J. R., Reid, J. S., Tackett, J. L., Vaughan, M. A., Zhang, J., and Marquis,
477 J. W.: Minimum aerosol layer detection sensitivities and their subsequent impacts on aerosol
478 optical thickness retrievals in CALIPSO level 2 data products, *Atmos. Meas. Tech.*, 11, 499-514,
479 <https://doi.org/10.5194/amt-11-499-2018>, 2018.
480
481 Toth, T. D., Zhang, J., Campbell, J. R., Hyer, E. J., Reid, J. S., Shi, Y., and Westphal, D. L.: Impact
482 of data quality and surface-to-column representativeness on the PM_{2.5} / satellite AOD relationship
483 for the contiguous United States, *Atmos. Chem. Phys.*, 14, 6049-6062,
484 <https://doi.org/10.5194/acp-14-6049-2014>, 2014.
485
486 Toth, T. D., Zhang, J., Campbell, J. R., Reid, J. S., and Vaughan, M. A.: Temporal variability of
487 aerosol optical thickness vertical distribution observed from CALIOP, *Journal of Geophysical*
488 *Research: Atmospheres*, 121(15), 9117-9139, <https://doi.org/10.1002/2015JD024668>, 2016.
489
490
491
492
493

494 **A bulk-mass-modeling-based method for retrieving Particulate Matter Pollution using**
495 **CALIOP observations**

496
497

498 Travis D. Toth¹, Jianglong Zhang², Jeffrey S. Reid³, and Mark A. Vaughan¹

499

500 ¹NASA Langley Research Center, Hampton, VA

501 ²Department of Atmospheric Sciences, University of North Dakota, Grand Forks, ND

502 ³Marine Meteorology Division, Naval Research Laboratory, Monterey, CA

503

504

505 *Correspondence to:* Travis D. Toth (travis.d.toth@nasa.gov); Jianglong Zhang

506 (jianglong.zhang@und.edu)

507

508

509 **Abstract.** In this proof-of-concept paper, we apply a bulk-mass-modeling method using
510 observations from the NASA Cloud-Aerosol Lidar with Orthogonal Polarization (CALIOP)
511 instrument for retrieving particulate matter (PM) concentration over the contiguous United States
512 (CONUS) over a 2-year period (2008-2009). Different from previous approaches that rely on
513 empirical relationships between aerosol optical depth (AOD) and PM_{2.5} (PM with particle
514 ~~diameters~~ less than 2.5 μm), for the first time, we derive PM_{2.5} concentrations, both at daytime and
515 nighttime, from near surface CALIOP aerosol extinction retrievals using bulk mass extinction
516 coefficients and model-based hygroscopicity. Preliminary results from this 2-year study
517 conducted over the CONUS show a good agreement ($r^2 \sim 0.48$; mean bias of $-3.3 \mu\text{g m}^{-3}$) between
518 the averaged nighttime CALIOP-derived PM_{2.5} and ground-based PM_{2.5} (with a lower r^2 of ~ 0.21
519 for daytime; mean bias of $-0.4 \mu\text{g m}^{-3}$), suggesting that PM concentrations can be obtained from
520 active-based spaceborne observations with reasonable accuracy. Results from sensitivity studies
521 suggest that accurate aerosol typing is needed for applying CALIOP measurements for PM_{2.5}
522 studies. Lastly, the e-folding correlation length for surface PM_{2.5} is found to be around 600 km for
523 the entire CONUS (~ 300 km for Western CONUS and ~ 700 km for Eastern CONUS), indicating

Deleted: sizes

525 that CALIOP observations, although sparse in spatial coverage, may still be applicable for PM_{2.5}
526 studies.

527

528 1 Introduction

529 During the last decade, an extensive number of studies have researched the feasibility of
530 estimating PM_{2.5} (particulate matter with particle ~~diameters~~ smaller than 2.5 μm) pollution with
531 the use of passive-based satellite-derived aerosol optical depth (AOD; e.g., Liu et al., 2007; Hoff
532 and Christopher, 2009; van Donkelaar et al., 2015). Monitoring of PM concentration from space
533 observations is needed, as PM_{2.5} pollution is one of the known causes of respiratory related diseases
534 as well as other health related issues (e.g., Liu et al., 2005; Hoff and Christopher, 2009; Silva et
535 al., 2013). Yet, ground-based PM_{2.5} measurements are often inconsistent or have limited
536 availability over much of the globe.

537 In some earlier studies, empirical relationships of PM_{2.5} concentrations and AODs were
538 developed and used for estimating PM_{2.5} concentrations from passive sensor retrieved AODs (e.g.,
539 Wang and Christopher, 2003; Engel-Cox et al., 2004; Liu et al., 2005; Kumar et al., 2007; Hoff
540 and Christopher, 2009). One of the limitations of this approach is that vertical distributions and
541 thermodynamic state of aerosol particles vary with space and time. Especially for regions with
542 elevated aerosol plumes, deep boundary layer entrainment zones, or strong nighttime inversions,
543 column-integrated AODs are not a good approximation of surface PM_{2.5} concentrations at specific
544 points and times (e.g., Liu et al., 2004; Toth et al., 2014; Reid et al., 2017). Indeed, Kaku et al.
545 (2018) recently showed that surface PM_{2.5} had longer spatial correlation lengths than AOD, even
546 in the “well behaved” southeastern United States where previous studies showed good [correlation](#)
547 [between PM_{2.5} and AOD](#) (e.g., Wang and Christopher, 2003). To account for variability in aerosol

Deleted: sizes

Deleted: performance

550 vertical distribution, several studies have attempted the use of chemical transport models, or CTMs
551 (e.g., van Donkelaar et al., 2015). Satellite data assimilation of AOD has become commonplace,
552 vastly improving AOD analyses and short-term prediction (e.g., Zhang et al., 2014; Sessions et al.,
553 2015). Yet, PM_{2.5} simulations remain poor (e.g., Reid et al., 2016). Uncertainties in such studies
554 are unavoidable due to uncertainties in CTM-based aerosol vertical distributions, and no nighttime
555 AODs are currently available from passive-based satellite retrievals.

556 It is arguable that from a climatological/long-term average perspective, the use of AOD as
557 a proxy for PM_{2.5} concentrations nevertheless has certain qualitative skill (e.g., Toth et al., 2014;
558 Reid et al., 2017) due to the averaging process that suppresses sporadic aerosol events with highly
559 variable vertical distributions. Still, as illustrated in Fig. 1, where 2-year (2008-2009) means of
560 Moderate Resolution Imaging Spectroradiometer (MODIS) AOD are plotted against PM_{2.5}
561 concentrations throughout the contiguous United States (CONUS), although a linear relationship
562 is plausibly shown, a low r^2 value of 0.08 is found. To construct Fig. 1, Aqua MODIS Collection
563 6 (C6) Optical_Depth_Land_And_Ocean data (0.55 μm), restricted to “Very Good” retrievals as
564 reported by the Land_Ocean_Quality_Flag, are first collocated with daily surface PM_{2.5}
565 measurements in both space and time (i.e., within 40 km in distance and the same day), and then
566 collocated daily pairs are averaged into 2-year means (for each PM_{2.5} site). Figure 1 may be
567 indicating that even from a long-term mean perspective, aerosol vertical distributions are not
568 uniform across the CONUS, which is also confirmed by other studies (e.g., Toth et al., 2014).
569 AOD retrievals themselves, with known uncertainties due to cloud contamination and assumptions
570 in the retrieval process (e.g., Levy et al., 2013), may also introduce uncertainties to that task.

571 On board the Cloud-Aerosol Lidar and Infrared Pathfinder Satellite Observations
572 (CALIPSO) satellite, the Cloud-Aerosol Lidar with Orthogonal Polarization (CALIOP) instrument

Deleted: for the most significant events as well as

Deleted: 9

575 provides observations of aerosol and cloud vertical distributions at both day and night (Hunt et al.,
576 2009; Winker et al., 2010). Given that CALIOP provides aerosol extinction retrievals near the
577 ground, it is interesting and reasonable to raise the question: can near surface CALIPSO extinction
578 be used as a better physical quantity than AOD for estimating surface $PM_{2.5}$ concentrations? This
579 is because unlike AOD, which is a column-integrated value, near surface CALIPSO extinction is,
580 in theory, a more realistic representation of near surface aerosol properties. Yet, in comparing
581 with passive sensors such as MODIS, which has a swath width on the order of ~ 2000 km, CALIOP
582 is a nadir pointing instrument with a narrow swath of ~ 70 m and a repeat cycle of 16 days (Winker
583 et al., 2009). Thus, the spatial sampling of CALIOP is sparse on a daily basis and temporal
584 sampling or other conditional or contextual biases are unavoidable if CALIOP observations are
585 used to estimate daily $PM_{2.5}$ concentrations (Zhang and Reid, 2009; Colarco et al., 2014). Also,
586 there are known uncertainties in CALIPSO retrieved extinction values due to uncertainties in the
587 retrieval process, such as the lidar ratio (extinction-to-backscatter ratio), calibration, and the
588 “retrieval fill value” (RFV) issue (Young et al., 2013; Toth et al., 2018).

589 Even with these known issues, especially the sampling bias, it is still compelling to
590 investigate if near surface CALIOP extinction can be utilized to retrieve surface $PM_{2.5}$
591 concentrations with reasonable accuracy from a long-term (i.e., two-year) mean perspective.
592 CALIOP data have been successfully used in $PM_{2.5}$ studies in the past, but primarily for assisting
593 passive-based AOD/ $PM_{2.5}$ analyses using aerosol vertical distribution as a constraint (e.g., Glantz
594 et al., 2009; van Donkelaar et al., 2010; Val Martin et al., 2013; Toth et al., 2014; Li et al., 2015;
595 Gong et al., 2017). However, the question remained as to the efficacy of the direct use of CALIOP
596 retrievals. To demonstrate a concept, we developed a bulk mass scattering scheme for inferring
597 PM concentrations from near surface aerosol extinction retrievals derived from CALIOP

598 observations. The bulk method used here is based upon the well-established relationship between
599 particle light scattering and $PM_{2.5}$ aerosol mass concentration (e.g., Charlson et al., 1968;
600 Waggoner and Weiss, 1980; Liou, 2002; Chow et al., 2006), discussed further, with the relevant
601 equations, in Sect. 2.

602 In this study, using two years (2008-2009) of CALIOP and United States (U.S.)
603 Environmental Protection Agency (EPA) data over the CONUS, the following questions are
604 addressed:

- 605 1. Can CALIOP extinction be used effectively for estimating $PM_{2.5}$ concentrations through a
606 bulk mass scattering scheme from a 2-year mean perspective for both daytime and
607 nighttime?
- 608 2. Can CALIOP extinction be used as a better parameter than AOD for estimating $PM_{2.5}$
609 concentrations from a 2-year mean perspective?
- 610 3. What are the sampling biases we can expect in CALIOP estimates of $PM_{2.5}$?
- 611 4. How do uncertainties in bulk properties compare to overall CALIOP-retrieved $PM_{2.5}$
612 uncertainty?

613 Details of the methods and datasets used are described in Sect. 2. Section 3 shows the
614 preliminary results using two years of EPA $PM_{2.5}$ and CALIOP data, including an uncertainty
615 analysis. The conclusions of this paper are provided in Sect. 4.

616

617

618

619 **2 Data and Methods**

620 Since 1970, the U.S. EPA has monitored surface PM using a number of Federal
621 Reference/Equivalent Methods (FRMs/FEMs), which employ gravimetric, tapered element
622 oscillating microbalance (TEOM), and beta gauge instruments (Federal Register, 1997;
623 Greenstone, 2002). Two years (2008-2009) of daily PM_{2.5} Local Conditions (EPA code = 88101)
624 data were acquired from the EPA Air Quality System for use in this investigation, consistent with
625 our previous PM_{2.5} study (Toth et al., 2014). These data represent PM_{2.5} concentrations over a 24-
626 hour period and include two scenarios: one sample is taken during the 24-hour duration (i.e., filter-
627 based measurement), or an average is computed from hourly samples within this time period (every
628 hour may not have an available measurement, however).

629 Note that uncertainties have been reported for hourly PM measurements (Kiss et al., 2017).
630 Examples of some uncertainties in these PM_{2.5} measurements depend upon the instrument/method
631 used: gravimetric (e.g., transport to the lab/human error and volatilization of PM during the drying
632 process; Patashnick et al., 2001), TEOM (e.g., errors due to improper inlet tube temperature;
633 Eatough et al., 2003), and beta attenuation monitors (e.g., changes in the sample flow rate due to
634 variations in temperature and moisture; Spagnolo, 1989). Also, it has been found that beta
635 attenuation monitors may be more accurate than TEOM, as TEOM can underestimate PM_{2.5} at low
636 temperatures (e.g., Chung et al., 2001). Still, as suggested by Kiss et al. (2017), PM data collected
637 over a longer period of time are much less likely to be biased. Thus, we expect lower uncertainties
638 from data collected over 24-hours, then daily data generated by averaging hourly observations.
639 Fully quantifying the differences from the two different PM observing methods, however, is the
640 subject for a future study.

641 CALIOP, flying aboard the CALIPSO platform within the A-Train satellite constellation,
642 is a dual wavelength (0.532 and 1.064 μm) lidar that has collected profiles of atmospheric aerosol

Deleted: We note that

Deleted: t

Deleted: Note that uncertainties have been reported for hourly PM measurements (Kiss et al., 2017). Examples of some uncertainties in these PM_{2.5} measurements depend upon the instrument/method used: gravimetric (e.g., transport to the lab/human error and volatilization of PM during the drying process; Patashnick et al., 2001), TEOM (e.g., errors due to improper inlet tube temperature; Eatough et al., 2003), and beta gauge (e.g., changes in the sample flow rate due to variations in temperature and moisture; Spagnolo, 1989). Also, it has been found that BAM may be more accurate than TEOM, as TEOM can underestimate PM_{2.5} at low temperatures (e.g., Chung et al., 2001). Still, as suggested by Kiss et al. (2017), PM data collected over a longer period of time are much less likely to be biased. Thus, we expected less uncertainties from data collected over 24-hours, then daily data generated by averaging hourly observations. Fully quantifying the differences from the two different PM observing methods, however is subject to a future study. ¶

662 particles and clouds since summer 2006 (Winker et al., 2007). In this study, daytime and nighttime
663 extinction coefficients retrieved at 0.532 μm from the Version 4.10 CALIOP Level 2 5 km aerosol
664 profile (L2_05kmAPro) product were used. Using parameters provided in the L2_05kmAPro
665 product, as well as the corresponding Level 2 5 km aerosol layer (L2_05kmALay) product, a robust
666 quality-assurance (QA) procedure for the aerosol observations was implemented (Table 1).
667 Further information on the QA metrics and screening protocol are discussed in detail in previous
668 studies (Kittaka et al. 2011; Campbell et al. 2012; Toth et al. 2013; 2016). Once the QA procedure
669 was applied, the aerosol profiles were linearly re-gridded from 60 m vertical resolution (above
670 mean sea level [AMSL]) to 100 m segments (i.e., resampled to 100 m resolution) referenced to the
671 local surface (above ground level [AGL]; Toth et al., 2014; 2016). The choice of 100 m was
672 arbitrary, and the profiles were re-gridded in order to obtain an AGL-corrected dataset, as opposed
673 to the AMSL-referenced profiles provided by the L2_05kmAPro product. Surface elevation and
674 relative humidity (RH) were taken from collocated model data included in the CALIPSO
675 L2_05kmAPro product (CALIPSO Data Products Catalog (Release 4.20); RH taken from the
676 Modern Era Retrospective-Analysis for Research, or MERRA-2 reanalysis product). To limit the
677 effects of signal attenuation and increase the chances of measuring aerosol presence near the
678 surface, the Atmospheric Volume Description parameter within the L2_05kmAPro dataset is used
679 to cloud-screen each aerosol profile as in Toth et al. (2018).

680 In this study, near surface PM mass concentration (C_m) is derived from near surface
681 CALIOP extinction based on a bulk formulation as in Equation 1 (e.g., Liou, 2002; Chow et al.,
682 2006):

683
$$\beta = C_m(a_{scat}f_{rh} + a_{abs}) \times 1000 \quad (1)$$

684 where β is CALIOP-derived near surface extinction in km^{-1} , C_m is the PM mass
685 concentration in $\mu\text{g m}^{-3}$, a_{scat} and a_{abs} are dry mass scattering and absorption efficiencies in $\text{m}^2 \text{g}^{-1}$,
686 and f_{rh} represents the light scattering hygroscopicity, respectively. As a preliminary study, for the
687 purpose of demonstrating this concept, we assume the dominant aerosol type over the contiguous
688 U.S. (CONUS) is pollution aerosol (i.e., the most prevalent near-surface aerosol type reported in
689 the CALIOP products for the CONUS during 2008-2009 is polluted continental) with a_{scat} and a_{abs}
690 values of 3.40 and $0.37 \text{ m}^2 \text{g}^{-1}$ (Hess et al., 1998; Lynch et al., 2016), respectively. These values
691 are similar to those reported in Malm and Hand (2007) and Kaku et al. (2018) but are interpolated
692 to $0.532 \mu\text{m}$ from values at $0.450 \mu\text{m}$ and $0.550 \mu\text{m}$ obtained from the Optical Properties of
693 Aerosols and Clouds (OPAC) model (Hess et al., 1998). Still, both a_{scat} and a_{abs} have regional and
694 species related dependencies. Also, only 2-year averages are used in this study, and we assume
695 that sporadic aerosol plumes are smoothed out in the averaging process, and that bulk aerosol
696 properties are similar throughout the study region. We have further explored the impact of aerosol
697 types to $\text{PM}_{2.5}$ retrievals in a later section. Furthermore, to aid in focusing this study on fine
698 mode/anthropogenic aerosols, those aerosol extinction range bins classified as dust by the CALIOP
699 typing algorithm were excluded from the analysis.

700 Also, surface PM concentrations are dry mass measurements. To account for the impact
701 of humidity on a_{scat} (it is assumed that a_{abs} is not affected by moisture; [Nessler et al., 2005](#); [Lynch](#)
702 [et al., 2016](#)), we estimated the hygroscopic growth factor for pollution aerosol based on Hanel
703 (1976), as shown in Equation 2:

$$704 \quad f_{rh} = \left(\frac{1 - RH}{1 - RH_{ref}} \right)^{-\Gamma} \quad (2)$$

705 where f_{rh} is the hygroscopic growth factor, RH is the relative humidity, and RH_{ref} is the
706 reference RH and is set to 30% in this study (Lynch et al., 2016). Γ is a unitless value (a fit
707 parameter describing the amount of hygroscopic increase in scattering) and is assumed to be 0.63
708 (i.e., sulfate aerosol) in this study (Hanel, 1976; Chew et al., 2016; Lynch et al., 2016).

709 Additionally, the CALIOP-derived PM density is for all particle sizes. To convert from
710 mass concentration of PM (C_m) to mass concentration of PM_{2.5} ($C_{m2.5}$), which represents mass
711 concentration for particle diameters smaller than 2.5 μm , we adopted the PM_{2.5} to PM₁₀ (PM with
712 diameters less than 10 μm) ratio (ϕ) of 0.6 as measured during the Studies of Emissions and
713 Atmospheric Composition, Clouds and Climate Coupling by Regional Surveys (SEAC⁴RS)
714 campaign over the US (Kaku et al., 2018). Again, the ratio of PM_{2.5} to PM₁₀ can also vary spatially,
715 however we used a regional mean to demonstrate the concept. Analyses in a later section using
716 two-years (2008-2009) of surface PM_{2.5} to PM₁₀ data suggest that 0.6 is a rather reasonable number
717 to use for the CONUS for the study period. Here we assume that mass concentrations for particle
718 diameters larger than 10 μm are negligible over the CONUS. Thus, we can rewrite Equation 1 as:

$$719 \quad C_{m2.5} = \frac{\beta \times \phi}{(a_{scat} \times f_{rh} + a_{abs}) \times 1000} \quad (3)$$

720 where $C_{m2.5}$ is the CALIOP-derived PM_{2.5} concentration in units of $\mu\text{g m}^{-3}$.

721 Lastly, we note that most of the results are shown in the form of scatter plots with fits from
722 Deming regression (Deming, 1943). Due to uncertainties in PM_{2.5} data, we show slopes computed
723 from Deming regression analyses instead of those from simple linear regression. Deming
724 regression in particular is appropriate here, as it accounts for errors in both the independent and
725 dependent variables (Deming, 1943), and has been used in past PM_{2.5} related studies (e.g., Huang
726 et al., 2014).

727

Deleted: Lastly

Deleted: sizes

Deleted: sizes

731 **3 Results and Discussion**

732 **3.1 Regional analysis**

733 Figure 2a shows the mean PM_{2.5} concentration using two years (2008-2009) of daily
734 surface PM_{2.5} data from the U.S. EPA (PM_{2.5_EPA}), not collocated with CALIOP observations. A
735 total of 1,091 stations (some operational throughout the entire period; others only partially) are
736 included in the analysis and observations from those stations are further used in evaluating
737 CALOP-derived PM_{2.5} concentrations (C_{m2.5}), as later shown in Fig. 3. PM_{2.5} concentrations of
738 ~10 µg m⁻³ are found over the eastern CONUS. In comparison, much lower PM_{2.5} concentrations
739 of ~5 µg m⁻³ are exhibited for the interior CONUS, over states including Montana, Wyoming,
740 North Dakota, South Dakota, Utah, Colorado, and Arizona. For the west coast of the CONUS,
741 and especially over California, higher PM_{2.5} concentrations are observed, with the maximum two-
742 year mean near 20 µg m⁻³. Note that the spatial distribution of surface PM_{2.5} concentrations over
743 the CONUS as shown in Fig. 2a is consistent with reported values from several studies (e.g., Hand
744 et al., 2013; Van Donkelaar et al., 2015; Di et al., 2017).

745 Figure 3a shows the two-year averaged 1° x 1° (latitude/longitude) gridded daytime
746 CALIOP aerosol extinction over the CONUS using CALIOP observations from 100-1000 m,
747 referenced to the number of cloud-free L2_05kmAPro profiles in each 1 x 1° bin. The lowest 100
748 m of CALIOP extinction data are not used in the analysis due to the potential of surface return
749 contamination (e.g., Toth et al., 2014), although this has been improved for the Version 4 CALIOP
750 products but may still be present in some cases. Here the averaged extinction from 100-1000 m is
751 used to represent near surface aerosol extinction. This selection of the 100-1000 m layer is
752 somewhat arbitrary, even though it is estimated from the mean CALIOP-based aerosol vertical
753 distribution over the CONUS (Toth et al., 2014). Thus, a sensitivity study is provided in a later

Deleted: , as surface layer heights may change seasonally and diurnally

756 section to understand the impact of this aerosol layer selection to CALIOP-based $PM_{2.5}$ retrievals.
757 As shown in Fig. 3a, higher mean near surface CALIOP extinction of 0.1 km^{-1} are found for the
758 eastern CONUS and over California, while lower values of $0.025\text{-}0.05 \text{ km}^{-1}$ found for the interior
759 CONUS. Figure 3b shows a plot similar to Fig. 3a but using nighttime CALIOP observations
760 only. Although similar spatial patterns are found during both day and night, the near surface
761 extinction values are overall lower for nighttime than daytime, and nighttime data are less noisy
762 than daytime. These findings are not surprising, as daytime CALIOP measurements are subject to
763 contamination from background solar radiation (e.g., Omar et al., 2013).

764 To investigate any diurnal biases in the data, Figs. 3c and 3d show the derived $PM_{2.5}$
765 concentration using daytime and nighttime CALIOP data respectively, based on the method
766 described in Section 2. Both Figures 3c and 3d suggest a higher $PM_{2.5}$ concentration of $\sim 10\text{-}12.5$
767 $\mu\text{g m}^{-3}$ over the eastern CONUS, and a much lower $PM_{2.5}$ concentration of $\sim 2.5\text{-}5 \mu\text{g m}^{-3}$ over the
768 interior CONUS. High $PM_{2.5}$ values of $10\text{-}20 \mu\text{g m}^{-3}$ are also found over the west coast of the
769 CONUS, particularly over California. The spatial distribution of $PM_{2.5}$ concentrations, as derived
770 using near surface CALIOP data (Figs. 3c and 3d, as well as the combined daytime and nighttime
771 perspective shown in Fig. 2c), is remarkably similar to the spatial distribution of $PM_{2.5}$ values as
772 estimated based on ground-based observations (Fig. 2a). Still, day and night differences in $PM_{2.5}$
773 concentrations are also clearly visible, as higher $PM_{2.5}$ values are found, in general, during daytime,
774 based on CALIOP observations. The high daytime $PM_{2.5}$ values, as shown in Fig. 3c, may
775 represent stronger near surface convection and more frequent anthropogenic activities during
776 daytime. However, they may also be partially contributed from solar radiation contamination.
777 Another possibility is that the daytime mean extinction coefficients (from which the mean $PM_{2.5}$
778 estimates are derived) appear artificially larger than at night due to high daytime noise limiting the

779 ability of CALIOP to detect fainter aerosol layers during daylight operations. Note that, for
780 context, maps of the number of days and CALIOP Level 2 5 km aerosol profiles used in the
781 creation of Fig. 3a-d are shown in Appendix Fig. 1.

782 Figure 3e shows the inter-comparison between $PM_{2.5_EPA}$ and $PM_{2.5_CALIOP}$ concentrations.
783 Note that only CALIOP and ground-based $PM_{2.5}$ data pairs, which are within 100 km of each other
784 and have reported values for the same day (i.e., year, month, and day), are used to generate Fig.
785 3e. Still, although only spatially and temporally collocated data pairs are used, ground-based $PM_{2.5}$
786 data represent 24-hour averages, while CALIOP-derived $PM_{2.5}$ concentrations are instantaneous
787 values over the daytime CALIOP overpass. To reduce this temporal bias, two years (2008-2009)
788 of collocated CALIOP-derived and measured $PM_{2.5}$ concentrations are averaged and only the two-
789 year averages are used in constructing Fig 3e. Also, to minimize the above-mentioned temporal
790 sampling bias, ground stations with fewer than 100 collocated pairs are discarded. This leaves a
791 total of 276 stations for constructing Fig. 3e.

792 As shown in Fig. 3e, an r^2 value of 0.21 (with slope of 1.07) is found between CALIOP-
793 derived and measured surface $PM_{2.5}$ concentrations, with a corresponding mean bias of $-0.40 \mu\text{g}$
794 m^{-3} ($PM_{2.5_CALIOP} - PM_{2.5_EPA}$). In comparison, Fig. 3f shows results similar to Fig. 3e, but for
795 nighttime CALIOP data. A much higher r^2 value of 0.48 (with slope of 0.96) is found between
796 CALIOP-derived and measurement $PM_{2.5}$ values from 528 EPA stations, with a corresponding
797 mean bias of $-3.3 \mu\text{g}\text{m}^{-3}$ ($PM_{2.5_CALIOP} - PM_{2.5_EPA}$). This may be related to the diurnal variability
798 of $PM_{2.5}$ concentrations, as the daily mean EPA measurement might be closer to the CALIOP A.M.
799 retrieval than to its P.M. counterpart. Still, data points are more scattered in Fig. 3e in comparison
800 with Fig. 3f, which again indicates that daytime CALIOP data are noisier, possibly due to daytime

Deleted: a
Deleted: 0.48

Deleted: a
Deleted: 0.67

805 solar contamination as well as other factors such as biases in relative humidity. Details of these
806 biases are further explored in Section 3.2.

807 To supplement this analysis, a pairwise $PM_{2.5_EPA}$ and $PM_{2.5_CALIOP}$ (day and night CALIOP
808 combined) analysis is presented in the spatial plots of Figs. 2b and 2d. Here, however, we lift the
809 100 collocated pairs requirement to increase data samples for better spatial representativeness. The
810 spatial variability of $PM_{2.5}$ over the CONUS is consistent with the observed patterns of non-
811 collocated data (i.e., Figs. 2a and 2c), but with generally higher values due to differences in
812 sampling. Also, comparing Figs. 2b and 2d, $PM_{2.5_EPA}$ spatial patterns match well with those of
813 $PM_{2.5_CALIOP}$, yet with larger values for $PM_{2.5_EPA}$ (consistent with the biases discussed above).
814 Lastly, a scatterplot of the pairwise analysis shown in Figs. 2b and 2d is provided in Fig. 4. An r^2
815 value of 0.40 is found between EPA and CALIOP-derived $PM_{2.5}$ concentrations from a combined
816 daytime and nighttime CALIOP perspective. Overall, Figs. 2, 3, and 4 indicate that near surface
817 CALIOP extinction data can be used to estimate surface $PM_{2.5}$ concentrations with reasonable
818 accuracy.

819

820 **3.2 Uncertainty analysis**

821 In this section, uncertainties in the CALIOP derived, 2-year averaged $PM_{2.5}$ concentrations
822 are explored as functions of aerosol vertical distribution, $PM_{2.5}$ to PM_{10} ratio, RH, aerosol type,
823 and cloud presence above. Spatial sampling related biases as well as prognostic errors are also
824 studied.

825

826 **3.2.1 Prognostic errors in $C_{m2.5}$**

827 As a first step for the uncertainty analysis, we estimated the prognostic error of 2-year
828 averaged $PM_{2.5_CALIOP}$. Figure 5 shows the root-mean-square error (RMSE) of CALIOP-based
829 $PM_{2.5}$ concentrations against those from EPA stations as a function of CALIOP-based $PM_{2.5}$ for
830 the 2008-2009 period over the CONUS. RMSEs were computed for five equally sampled bins,
831 determined from a cumulative histogram analysis. Each point in Fig. 5, from left to right,
832 represents the RMSE and mean $PM_{2.5}$ concentration derived from CALIOP for 0-20%, 20-40%,
833 40-60%, 60-80%, and 80-100% cumulative frequencies. A mean combined daytime and nighttime
834 RMSE of $\sim 4 \mu g m^{-3}$ is found, with a mean value slightly greater for nighttime ($\sim 4.3 \mu g m^{-3}$) than
835 daytime ($\sim 3.7 \mu g m^{-3}$). While most bins exhibit larger nighttime RMSEs, daytime RMSEs are
836 larger for the greatest mean CALIOP-derived $PM_{2.5}$ concentrations.

Deleted: RMSEs were computed in intervals of $5 \mu g m^{-3}$ from 0 to $25 \mu g m^{-3}$, with no computations greater than $25 \mu g m^{-3}$ performed due to very few data points above this $PM_{2.5}$ concentration level.

Deleted: minimum error

Deleted: with

837
838
839 **3.2.2 Surface layer height sensitivity study**

840 A sensitivity study was conducted for which $PM_{2.5}$ was derived from near-surface CALIOP
841 aerosol extinction by varying the height of the surface layer in increments of 100 m from the
842 ground to 1000 m. Note that the surface layer (0-100 m) is included for this sensitivity study only.
843 The statistical results of this analysis, for both daytime and nighttime conditions, are shown in
844 Table 2. Four statistical parameters were computed, consisting of r^2 , slope from Deming
845 regression, mean bias (CALIOP – EPA) of $PM_{2.5}$, and percent error change in derived $PM_{2.5}$,
846 defined as: $((\text{mean_new_}PM_{2.5} - \text{mean_original_}PM_{2.5}) / \text{mean_original_}PM_{2.5}) * 100$. For context,
847 the bottom row of Table 2 shows the results from the original analysis. In terms of r^2 and slope,
848 optimal values peak at different surface layer heights between daytime and nighttime. For
849 example, for daytime, the largest correlations are found for the 0-600 m and 0-700 m layers, while

Deleted: generally larger RMSEs for nighttime below $15 \mu g m^{-3}$, and larger RMSEs for daytime above $15 \mu g m^{-3}$. However, mean RMSEs (i.e., computed from the RMSEs shown in Fig. 5) are similar for both datasets, $\sim 4.5 \mu g m^{-3}$ for daytime and $\sim 4.0 \mu g m^{-3}$ for nighttime. Also, note that while the absolute error for daytime is largest at high $PM_{2.5}$ concentrations, relative errors are similar (e.g., $3 \mu g m^{-3} / 10 \mu g m^{-3}$ or 30% for the 5-10 $\mu g m^{-3}$ bin, versus $7 \mu g m^{-3} / 25 \mu g m^{-3}$ or 28% for the 20-25 $\mu g m^{-3}$ bin). For context, the number of samples per bin are also plotted (as X symbols) in Fig. 5. Data sample sizes are smallest (largest) for the lowest/highest range (mid-range) $PM_{2.5}$ bins.

Deleted: , slope

867 for nighttime these are found for the 0-300 m and 0-400 m layers. However, the 0-300 m layer
868 exhibits the lowest mean bias for the daytime analysis, and the 100-1000 m layer exhibits the
869 lowest mean bias for the nighttime analysis. Overall, marginal changes are found for varying the
870 height of the surface layer. Yet the largest mean bias is found for the 0-100 m layer, indicating
871 the need for excluding the 0-100 m layer in the analysis.

872

873 3.2.3 RH sensitivity study

874 Profiles of RH were taken from the MERRA-2 reanalysis product, as these collocated data
875 are provided in the CALIPSO L2_05kmAPro product. However, biases may exist in this RH
876 dataset. Thus, we examined the impact of varying the RH values by +/- 10% on the CALIOP-
877 derived PM_{2.5} concentrations. For both daytime and nighttime analyses, no significant differences
878 in the r² and slope values were found. However, a +15% change in the mean derived PM_{2.5} values
879 was found by decreasing the RH values by 10%, while a -15% change in the mean derived PM_{2.5}
880 values was found by increasing the RH values by 10%.

881 3.2.4 PM_{2.5} to PM₁₀ ratio sensitivity study

882 Another source of uncertainty in this study is the PM_{2.5}/PM₁₀ ratio. Using surface-based
883 PM_{2.5} and PM₁₀ data from those EPA stations over the CONUS for 2008-2009 with concurrent
884 PM_{2.5} and PM₁₀ daily data available (i.e., 409 stations), we computed the mean PM_{2.5}/PM₁₀ ratio,
885 and its corresponding standard deviation. The mean ratio was 0.56 with a standard deviation of
886 0.32. It is interesting to note that the mean PM_{2.5}/PM₁₀ ratio estimated from two years of surface
887 observations over the CONUS is close to 0.6 (the number used in this study), as reported by Kaku
888 et al. (2018). We also tested the sensitivity of the derived PM_{2.5} concentrations as a function of
889 PM_{2.5}/PM₁₀ ratio for two scenarios: ±1 standard deviation of the mean (Table 3). In general, a ±50

Deleted: (100-1000 m layer)

Deleted: (

Deleted:)

Formatted: Indent: First line: 0.5"

Deleted:

Deleted: However, a +15% (-15%) change in the mean derived PM_{2.5} values was found by decreasing (increasing) the RH values by 10%.

Formatted: Subscript

Formatted: Subscript

897 % to 60 % change is found with the variation of the $PM_{2.5}/PM_{10}$ ratio at the range of ± 1 standard
898 deviation of the mean. As suggested from Table 3, the lowest mean daytime bias is found for a
899 ratio of 0.6, and for nighttime the lowest mean bias occurs using a ratio of 0.88.

Deleted: , the optimal slope is found using a ratio of +1 standard deviation of the mean for both daytime and nighttime.

Deleted: T

900

901 3.2.5 Sampling-related biases

902 As mentioned in the introduction section, a sampling bias, due to the very small footprint
903 size and ~ 16 day repeat cycle of CALIOP, can exist when using CALIOP observations for $PM_{2.5}$
904 estimates (Zhang and Reid, 2009). This sampling-induced bias is investigated from a 2-year mean
905 perspective by comparing histograms of $PM_{2.5_EPA}$ and $C_{m2.5}$ concentrations as shown in Fig. 6. To
906 generate Fig. 6, all available daily EPA $PM_{2.5}$ are used to represent the “true” 2-year mean spectrum
907 of $PM_{2.5}$ concentrations over the EPA sites. The aerosol extinction data spatially collocated to the
908 EPA sites (Sect. 3.1), but not temporally collocated, are used for estimating the 2-year mean
909 spectrum of $PM_{2.5}$ concentrations as derived from CALIOP observations. To be consistent with
910 the previous analysis, only cloud-free CALIOP profiles are considered. The $PM_{2.5_EPA}$
911 concentrations peak at $\sim 10 \mu g m^{-3}$ (standard deviation of $\sim 3 \mu g m^{-3}$), and CALIOP-derived $PM_{2.5}$
912 peaks at $\sim 9 \mu g m^{-3}$ (daytime; standard deviation of $\sim 4 \mu g m^{-3}$) and $\sim 7 \mu g m^{-3}$ (nighttime; standard
913 deviation of $\sim 2 \mu g m^{-3}$). The distribution shifts towards smaller concentrations for CALIOP, more
914 so for nighttime than daytime (possibly due to CALIOP daytime versus nighttime detection
915 differences).

Deleted: 9

Deleted: 5

916 Still, Fig. 6 may reflect the diurnal difference in $PM_{2.5}$ concentrations as well as the
917 retrieval bias in $C_{m2.5}$ values. Thus, we have re-performed the exercise shown in Fig. 6 using
918 spatially and temporally collocated $PM_{2.5_EPA}$ and $C_{m2.5}$ data as shown in Fig. 7. To construct Fig.
919 7, $PM_{2.5_EPA}$ and $C_{m2.5}$ data are collocated following the steps mentioned in Sect. 3.1, with CALIOP

925 and EPA PM_{2.5} representing 2-year mean values for each EPA station. Again, only cloud-free
926 CALIOP profiles are considered for this analysis. As shown in Fig. 7a, the PM_{2.5_EPA}
927 concentrations peak at $\sim 12 \mu\text{g m}^{-3}$ (standard deviation of $\sim 4 \mu\text{g m}^{-3}$), and daytime C_{m2.5} peaks at
928 $\sim 10 \mu\text{g m}^{-3}$ (standard deviation of $\sim 4 \mu\text{g m}^{-3}$). In comparison, with the use of collocated nighttime
929 C_{m2.5} and PM_{2.5_EPA} data as shown in Fig. 7b, the peak PM_{2.5_EPA} value is about $5 \mu\text{g m}^{-3}$ higher
930 than the peak C_{m2.5} value (with similar standard deviations as found in the analyses of Fig. 7a).
931 Considering both Figs. 6 and 7, it is likely that the temporal sampling bias seen in Fig. 6 is at least
932 in part due to retrieval bias as well as the difference in PM_{2.5} concentrations during daytime and
933 nighttime.

Deleted: 7

Deleted: 6

Deleted: 2

934

935 3.2.6 CALIOP AOD analysis

936 Most past studies focused on the use of column AODs as proxies for surface PM_{2.5} (e.g.,
937 Liu et al., 2005; Hoff and Christopher, 2009; van Donkelaar et al., 2015). Therefore, it is
938 interesting to investigate whether near surface CALIOP extinction values can be used as a better
939 physical quantity to estimate surface PM_{2.5} in comparing with column-integrated CALIOP AOD.
940 To achieve this goal, we have compared CALIOP column AOD and PM_{2.5} from EPA stations, as
941 shown in Fig. 8. Similar to the scatterplots of Fig. 4, each point represents a two-year mean for
942 each EPA site, and was created from a dataset following the same spatial/temporal collocation as
943 described above. As shown in Fig. 9, r² values of 0.04 and 0.13 are found using CALIOP daytime
944 and nighttime AOD data, respectively, similar to the MODIS-based analysis shown in Fig. 1. This
945 is expected, as elevated aerosol layers will negatively impact the relationship between surface
946 PM_{2.5} and column AOD. The derivation of surface PM_{2.5} from near surface CALIOP extinction,
947 as demonstrated from this study however, provides a much better spatial matching between the

951 quantities being compared, with potential error terms that can be well quantified and minimized in
952 later studies.

953

954 3.2.7 Cloud flag sensitivity study

955 For most of this paper, a strict cloud screening process is implemented, during which no
956 clouds are allowed in the entire CALIOP profile. However, in contrast to passive sensor
957 capabilities (e.g., MODIS), near-surface aerosol extinction coefficients can be readily retrieved
958 from CALIOP profiles even when there are transparent cloud layers above. Therefore, we
959 conducted an additional analysis for which no cloud flag was set (i.e., all-sky conditions). Results

960 are shown in scatterplot form in Fig. 9, in a similar manner as Figs. 3e and f, ~~with an additional 97~~

961 ~~points for the daytime analysis and 156 points for the nighttime analysis.~~ Comparing the all-sky

962 results with those of Figs. 3e, and f (cloud-free conditions), the r^2 values are similar. This is also

963 true in terms of mean bias, with similar values of $0.70 \mu\text{g m}^{-3}$ found for daytime, ~~and $-2.68 \mu\text{g m}^{-3}$~~

964 ~~for nighttime, all-sky scenarios.~~ This indicates that our method performs reasonably well from an

965 all-sky perspective. However, we note that restricting the analysis to solely those cases that are

966 cloudy (not shown), the method does not perform as well. For example, the r^2 value, ~~decreases by~~

967 ~~71% for the daytime analysis compared to the cloud-free results (Fig. 3e). The corresponding~~

968 ~~nighttime r^2 value decreases by 90%.~~ This is expected, as any errors made in estimating the optical

969 depths of the overlying clouds will propagate (as biases) into the extinction retrievals for the

970 underlying aerosols.

971

972 3.2.8 Aerosol type analysis

Deleted: with an additional 97 (156) points for the daytime (nighttime) analyses

Deleted: .

Deleted: (-2.68)

Deleted:

Deleted: (nighttime)

Deleted:

Deleted: s

Deleted: (

Deleted:)

Deleted: and the slope values decrease by 21% (75%) for the daytime (nighttime) analyses, compared to the cloud-free results (Figs. 3e and f).

986 Also, for this study, we assume that the primary aerosol type over the CONUS is pollution
987 (i.e., sulfate) aerosol, which is generally composed of smaller (fine mode) particles that tend to
988 exhibit mass extinction efficiencies $\sim 4 \text{ m}^2 \text{ g}^{-1}$. However, even after implementing our dust-free
989 restriction, the study region can also be contaminated with non-pollution aerosols, which can have
990 a larger particle size and exhibit lower mass extinction efficiencies (e.g., Hess et al., 1998; Malm
991 and Hand, 2007; Lynch et al., 2016). The use of $\text{PM}_{2.5}$ versus PM_{10} somewhat mitigates this size
992 dependency, but nevertheless coarse mode dust or sea salt can dominate $\text{PM}_{2.5}$ mass values (e.g.,
993 Atwood et al., 2013).

Deleted: & organic

994 Thus, in this section, the impact of aerosol types to the derived $\text{PM}_{2.5}$ concentrations was
995 explored by varying the mass scattering and absorption efficiencies and gamma values associated
996 with each aerosol type. The three aerosol types chosen for this sensitivity study were dust, sea
997 salt, and smoke, based upon Lynch et al. (2016). The mass scattering and absorption values for
998 dust and sea salt were interpolated to $0.532 \mu\text{m}$ from values at $0.450 \mu\text{m}$ and $0.550 \mu\text{m}$ from OPAC
999 (as was done for the sulfate case; Hess et al., 1998). For smoke, these values were interpolated to
1000 $0.532 \mu\text{m}$ from values at $0.440 \mu\text{m}$ and $0.670 \mu\text{m}$ as provided by Reid et al. (2005) for smoke cases
1001 over the US and Canada. The gamma values were taken from Lynch et al. (2016) and the
1002 references within. These values, as well as the results from this sensitivity study, are shown in
1003 Table 4. If we assume all aerosols within the study region are smoke aerosols, no major changes
1004 in the retrieved CALIOP $\text{PM}_{2.5}$ values are found. However, significant uncertainties on the order
1005 of $\sim 200\%$ are found if sea salt, or $\sim 800\%$ if dust, aerosol mass scattering/absorption efficiencies
1006 and gamma values are used instead. Clearly, this study suggests that accurate aerosol typing is
1007 necessary for future applications of CALIOP observations for surface $\text{PM}_{2.5}$ estimations.

Deleted: ($\sim 800\%$)

Deleted: (

Deleted:)

1008

1013 **3.3 E-folding correlation length for PM_{2.5} concentrations over the CONUS**

Deleted: 2.9

1014 As a last study, we also estimated the spatial e-folding correlation length for PM_{2.5}
1015 concentrations over the CONUS. This provides us an estimation of the correlation between a
1016 CALIOP-derived and actual PM_{2.5} concentration for a given location as a function of distance
1017 between the CALIOP observation and the given location. To accomplish this, all EPA stations
1018 over the CONUS with at least 50 days of daily data available for the 2008-2009 period were first
1019 determined. Next, the distances between each pair of these EPA stations, and their corresponding
1020 correlation of daily PM_{2.5} concentrations, were computed. Results are shown in Fig. 10 as a
1021 scatterplot, with individual points in gray and the black curve representing the exponential fit to
1022 the data. A decrease in PM_{2.5} correlation with distance between EPA stations is found, and the e-
1023 folding length in correlation (e.g., correlation reduced to 1/e, or 0.37) is ~600 km (from an AOD
1024 standpoint, this value is 40-400 km, as suggested by Anderson et al., 2003).

1025 Also included in Fig. 10 are results from a corresponding regional analysis, with the red
1026 and blue lines showing bin averages (10 km) for the Western and Eastern CONUS, respectively
1027 (regions partitioned by the -97° longitude line). The e-folding length is ~300 km for the Western
1028 CONUS, and ~700 km for the Eastern CONUS, indicating a much shorter correlation length for
1029 pollution over the Western CONUS, possibly due to a more complex terrain such as mountains.
1030 Overall, these PM_{2.5} e-folding lengths suggest that CALIOP-derived PM_{2.5} concentrations could
1031 still have some representative skill within a few hundred kilometers of a given location.

Deleted: (

Deleted:)

Deleted: Western (

Deleted:)

1032

1033 **4 Conclusions**

1034 In this paper, we have demonstrated a new bulk-mass-modeling method for retrieving
1035 surface particulate matter (PM) with particle diameters smaller than 2.5 μm (PM_{2.5}) using

Deleted: sizes

1042 observations acquired by the NASA Cloud-Aerosol Lidar with Orthogonal Polarization (CALIOP)
1043 instrument from 2008-2009. For the purposes of demonstrating this concept, only regionally-
1044 averaged parameters, such as mass scattering and absorption coefficients, and PM_{2.5} to PM₁₀ (PM
1045 with particle diameters smaller than 10 μm) conversion ratio, are used. Also, we assume the
1046 dominant type of aerosols over the study region is pollution aerosols (supported by the occurrence
1047 frequencies of aerosol types determined by the CALIOP algorithms), and exclude aerosol
1048 extinction range bins classified as dust from the analysis. Even with the highly-averaged
1049 parameters, the results from this paper are rather promising and demonstrate a potential for
1050 monitoring PM pollution using active-based lidar observations. Specifically, the primary results
1051 of this study are as follows:

Deleted: sizes

- 1052 1. CALIOP-derived PM_{2.5} concentrations of ~10-12.5 μg m⁻³ are found over the eastern
1053 contiguous United States (CONUS), with lower values of ~2.5-5 μg m⁻³ over the central
1054 CONUS. PM_{2.5} values of ~10-20 μg m⁻³ are found over the west coast of the CONUS,
1055 primarily California. The spatial distribution of 2-year mean PM_{2.5} concentrations derived
1056 from near surface CALIOP aerosol data compares well to the spatial distribution of *in situ*
1057 PM_{2.5} measurements collected at the ground-based stations of the U.S. Environmental
1058 Protection Agency (EPA). The use of nighttime CALIOP extinction to derive PM_{2.5} results
1059 in a higher correlation ($r^2 = 0.48$; mean bias = -3.3 μgm⁻³) with EPA PM_{2.5} than daytime
1060 CALIOP extinction data ($r^2 = 0.21$; mean bias = -0.40 μgm⁻³).
- 1061 2. Correlations between CALIOP aerosol optical depth (AOD) and EPA PM_{2.5} are much
1062 lower (r^2 values of 0.04 and 0.13, for daytime and nighttime CALIOP AOD data,
1063 respectively) than those obtained from derived PM_{2.5} using near-surface CALIOP aerosol
1064 extinction. A similar correlation is also found between Moderate Resolution Imaging

1066 Spectroradiometer (MODIS) AOD and EPA PM_{2.5} from two-year (2008-2009) means.
1067 This suggests that CALIOP extinction may be used as a better parameter for estimating
1068 PM_{2.5} concentrations from a 2-year mean perspective. Also, the algorithm proposed in this
1069 study is essentially a semi-physical-based method, and thus the retrieval process can be
1070 improved, upon a careful study of the physical parameters used in the process.

1071 3. Spatial and temporal sampling biases, as well as a retrieval bias, are found. Also, several
1072 sensitivity studies were conducted, including surface layer height, cloud flag, PM_{2.5}/PM₁₀
1073 ratio, relative humidity, and aerosol type. The sensitivity studies highlight the need for
1074 accurate aerosol typing for estimating PM_{2.5} concentrations using CALIOP observations.

1075 4. Using surface-based PM_{2.5} at EPA stations alone, the e-folding correlation length for PM_{2.5}
1076 concentrations was found to be about 600 km for the CONUS. A regional analysis yielded
1077 values of ~300 km and ~700 km for the Western and Eastern CONUS, respectively. Thus,
1078 while limited in spatial sampling, measurements from CALIOP may still be used for
1079 estimating PM_{2.5} concentrations over the CONUS.

1080 As noted earlier, CALIOP observations are still rather sparse, and concerns related to
1081 reported CALIOP aerosol extinction values also exist, such as solar and surface contamination and
1082 the “retrieval fill value” issue (e.g., Toth et al., 2018). Yet, the future High Spectral Resolution
1083 Lidar (HSRL) instrument on board the Earth Clouds, Aerosol, and Radiation Explorer
1084 (EarthCARE) satellite (Illingworth et al., 2015), as well as forthcoming space-based lidar missions
1085 in response to the 2017 Decadal Survey, offer opportunities to further explore aerosol extinction -
1086 based PM concentrations. Ultimately the results from this study show that the combined use of
1087 several lidar instruments for monitoring regional and global PM pollution is potentially achievable.

1088

1089 **Acknowledgements**

1090 This research was funded with the support of the NASA Earth and Space Science Fellowship
1091 program (NNX16A066H). Author JZ acknowledges the support from NASA grant
1092 NNX17AG52G. CALIPSO data were obtained from the NASA Langley Research Center
1093 Atmospheric Science Data Center (eos-web.larc.nasa.gov). MODIS data were obtained from
1094 NASA Goddard Space Flight Center (ladsweb.nascom.nasa.gov). The PM_{2.5} data were obtained
1095 from the EPA AQS site (https://aqs.epa.gov/aqsweb/airdata/download_files.html).

1096

1097

1098

1099

1100

1101

1102

1103

1104

1105

1106

1107

1108

1109

1110 **References**

1111

- 1112 Anderson, T.L., Charlson, R. J., Winker, D.M., Ogren, J.A., and Holmén, K.: Mesoscale
1113 Variations of Tropospheric Aerosols, *J. Atmos. Sci.*, 60, 119–136,
1114 [https://doi.org/10.1175/1520-0469\(2003\)060<0119:MVOTA>2.0.CO;2](https://doi.org/10.1175/1520-0469(2003)060<0119:MVOTA>2.0.CO;2), 2003.
- 1115 Atwood, S. A., J. S. Reid, S. M. Kreidenweis, S. S. Cliff, Y. Zhao, N.-H. Lin, S.-C. Tsay, Y.-C.
1116 Chu, and Westphal, D.L.: Size resolved measurements of springtime aerosol particles over
1117 the northern South China Sea, *Atmospheric Environment*, 78, 134-143,
1118 <https://doi.org/10.1016/j.atmosenv.2012.11.024>, 2013.
- 1119 Campbell, J. R., Tackett, J. L., Reid, J. S., Zhang, J., Curtis, C. A., Hyer, E. J., Sessions, W. R.,
1120 Westphal, D. L., Prospero, J. M., Welton, E. J., Omar, A. H., Vaughan, M. A., and Winker,
1121 D. M.: Evaluating nighttime CALIOP 0.532 μm aerosol optical depth and extinction
1122 coefficient retrievals, *Atmos. Meas. Tech.*, 5, 2143-2160, [https://doi.org/10.5194/amt-5-](https://doi.org/10.5194/amt-5-2143-2012)
1123 [2143-2012](https://doi.org/10.5194/amt-5-2143-2012), 2012.
- 1124 Charlson, R. J., Ahlquist, N. C., and Horvath, H.: On the generality of correlation of atmospheric
1125 aerosol mass concentration and light scatter, *Atmospheric Environment*, 2(5), 455-464,
1126 [https://doi.org/10.1016/0004-6981\(68\)90039-5](https://doi.org/10.1016/0004-6981(68)90039-5), 1968.
- 1127 Chew, B. N., Campbell, J. R., Hyer, E. J., Salinas, S. V., Reid, J. S., Welton, E. J., Holben, B.N.
1128 and Liew, S. C.: Relationship between aerosol optical depth and particulate matter over
1129 Singapore: Effects of aerosol vertical distributions, *Aerosol and Air Quality Research*, 16,
1130 2818-2830, <https://doi.org/10.4209/aaqr.2015.07.0457>, 2016.
- 1131 Chow, J. C., Watson, J. G., Park, K., Robinson, N. F., Lowenthal, D. H., Park, K., and Magliano,
1132 K. A.: Comparison of particle light scattering and fine particulate matter mass in central
1133 California, *Journal of the Air & Waste Management Association*, 56(4), 398-410,
1134 <https://doi.org/10.1080/10473289.2006.10464515>, 2006.

1135
1136 [Chung, A., Chang, D. P., Kleeman, M. J., Perry, K. D., Cahill, T. A., Dutcher, D., ... & Stroud, K.:](#)
1137 [Comparison of real-time instruments used to monitor airborne particulate matter, *Journal*](#)
1138 [of the Air & Waste Management Association, 51\(1\), 109-120, 2001.](#)

1139 Colarco, P. R., Kahn, R. A., Remer, L. A., and Levy, R. C.: Impact of satellite viewing-
1140 swath width on global and regional aerosol optical thickness statistics and trends, *Atmos.*
1141 *Meas. Tech.*, 7, 2313-2335, <https://doi.org/10.5194/amt-7-2313-2014>, 2014.

1142 [Deming, W.E.: *Statistical Adjustment of Data*, Wiley: New York, 1943.](#)

1143 Di, Q., Wang, Y., Zanobetti, A., Wang, Y., Koutrakis, P., Choirat, C., ... and Schwartz, J. D.: Air
1144 pollution and mortality in the Medicare population, *New England Journal of*
1145 *Medicine*, 376(26), 2513-2522, doi: 10.1056/NEJMoa170274, 2017.

1146 [Eatough, D. J., Long, R. W., Modey, W. K., and Eatough, N. L.: *Semi-volatile secondary organic*](#)
1147 [aerosol in urban atmospheres: meeting a measurement challenge, *Atmospheric*](#)
1148 [Environment, 37\(9-10\), 1277-1292, 2003.](#)

1149 Engel-Cox, J. A., Holloman, C. H., Coutant, B. W., and Hoff, R. M.: Qualitative and quantitative
1150 evaluation of MODIS satellite sensor data for regional and urban scale air quality, *Atmos.*
1151 *Environ.*, 38, 2495–2509, <https://doi.org/10.1016/j.atmosenv.2004.01.039>, 2004.

1152 Federal Register: National ambient air quality standards for particulate matter. Final Rule
1153 Federal Register/vol. 62, no. 138/18 July 1997/Final Rule, 40 CFR Part 50, 1997.

1154 Glantz, P., Kokhanovsky, A., von Hoyningen-Huene, W., and Johansson, C.: Estimating
1155 PM2.5 over southern Sweden using space-borne optical measurements, *Atmospheric*
1156 *Environment*, 43(36), 5838-5846, <https://doi.org/10.1016/j.atmosenv.2009.05.017>, 2009.

1157 Gong, W., Huang, Y., Zhang, T., Zhu, Z., Ji, Y., and Xiang, H.: Impact and Suggestion of

1158 Column-to-Surface Vertical Correction Scheme on the Relationship between Satellite
1159 AOD and Ground-Level PM_{2.5} in China, *Remote Sensing*, 9(10), 1038,
1160 <https://doi.org/10.3390/rs9101038>, 2017.

1161 Greenstone, M.: The impacts of environmental regulations on industrial activity: Evidence from
1162 the 1970 and 1977 clean air act amendments and the census of manufactures, *Journal of*
1163 *political economy*, 110(6), 1175-1219, <https://doi.org/10.1086/342808>, 2002.

1164 Hand, J. L., and Malm, W. C.: Review of aerosol mass scattering efficiencies from ground-
1165 based measurements since 1990, *Journal of Geophysical Research:*
1166 *Atmospheres*, 112(D16), <https://doi.org/10.1029/2007JD008484>, 2007.

1167 Hand, J. L., Schichtel, B. A., Malm, W. C., and Frank, N. H.: Spatial and temporal trends in PM_{2.5}
1168 organic and elemental carbon across the United States, *Advances in*
1169 *Meteorology*, <http://dx.doi.org/10.1155/2013/367674>, 2013.

1170 Hänel, G.: The properties of atmospheric aerosol particles as functions of the relative humidity at
1171 thermodynamic equilibrium with the surrounding moist air, *Advances in geophysics*, 19,
1172 73-188, [https://doi.org/10.1016/S0065-2687\(08\)60142-9](https://doi.org/10.1016/S0065-2687(08)60142-9), 1976.

1173 Hess, M., Koepke, P., and Schult, I.: Optical properties of aerosols and clouds: The software
1174 package OPAC, *Bulletin of the American meteorological society*, 79(5), 831-844,
1175 [https://doi.org/10.1175/1520-0477\(1998\)079%3C0831:OPOAAC%3E2.0.CO;2](https://doi.org/10.1175/1520-0477(1998)079%3C0831:OPOAAC%3E2.0.CO;2), 1998.

1176 Hoff, Raymond M., and Christopher, Sundar A.: Remote sensing of particulate pollution from
1177 space: have we reached the promised land?, *Journal of the Air & Waste Management*
1178 *Association*, 59.6 (2009): 645-675, <https://doi.org/10.3155/1047-3289.59.6.645>, 2009.

1179 [Huang, X. H., Bian, Q., Ng, W. M., Louie, P. K., and Yu, J. Z.: Characterization of PM_{2.5} major](#)

1180 [components and source investigation in suburban Hong Kong: a one year monitoring](#)
1181 [study, *Aerosol Air Qual. Res.* 14\(1\), 237-250, 2014.](#)

1182 Hunt, W. H., Winker, D. M., Vaughan, M. A., Powell, K. A., Lucker, P. L., and Weimer, C.:
1183 CALIPSO lidar description and performance assessment, *Journal of Atmospheric and*
1184 *Oceanic Technology*, 26(7), 1214-1228, <https://doi.org/10.1175/2009JTECHA1223.1>,
1185 2009.

1186 Illingworth, Anthony J., et al.: The EarthCARE satellite: The next step forward in global
1187 measurements of clouds, aerosols, precipitation, and radiation, *Bulletin of the American*
1188 *Meteorological Society*, 96.8, 1311-1332, <https://doi.org/10.1175/BAMS-D-12-00227.1>,
1189 2015.

1190 Kaku, K. C., Reid, J. S., Hand, J. L., Edgerton, E. S., Holben, B. N., Zhang, J., and Holz, R. E.:
1191 Assessing the challenges of surface-level aerosol mass estimates from remote sensing
1192 during the SEAC4RS and SEARCH campaigns: Baseline surface observations and remote
1193 sensing in the southeastern United States, *Journal of Geophysical Research: Atmospheres*,
1194 123, 7530–7562, <https://doi.org/10.1029/2017JD028074>, 2018.

1195 [Kiss, G., Imre, K., Molnár, Á., and Gelencsér, A.: Bias caused by water adsorption in hourly PM](#)
1196 [measurements, *Atmos. Meas. Tech.*, 10, 2477-2484, \[https://doi.org/10.5194/amt-10-2477-\]\(https://doi.org/10.5194/amt-10-2477-2017\)](#)
1197 [2017, 2017.](#)

1198 Kittaka, C., Winker, D. M., Vaughan, M. A., Omar, A., & Remer, L. A.: Intercomparison of
1199 column aerosol optical depths from CALIPSO and MODIS-Aqua, *Atmospheric*
1200 *Measurement Techniques*, 4(2), 131, <https://doi.org/10.5194/amt-4-131-2011>, 2011.

1201 Kumar, N., Chu, A., and Foster, A.: An empirical relationship between PM2.5 and aerosol optical

1202 depth in Delhi Metropolitan, *Atmos. Environ.*, 41, 4492–4503,
1203 <https://doi.org/10.1016/j.atmosenv.2007.01.046>, 2007.

1204 Levy, R. C., Mattoo, S., Munchak, L. A., Remer, L. A., Sayer, A. M., Patadia, F., and Hsu, N.C.:
1205 The Collection 6 MODIS aerosol products over land and ocean, *Atmos. Meas. Tech.*, 6,
1206 2989-3034, <https://doi.org/10.5194/amt-6-2989-2013>, 2013.

1207 Li, J., Carlson, B. E., and Laciš, A. A.: How well do satellite AOD observations represent the
1208 spatial and temporal variability of PM_{2.5} concentration for the United States?,
1209 *Atmospheric environment*, 102, 260-273, <https://doi.org/10.1016/j.atmosenv.2014.12.010>,
1210 2015.

1211 Liu, Y., Franklin, M., Kahn, R., and Koutrakis, P.: Using aerosol optical thickness to predict
1212 ground-level PM_{2.5} concentrations in the St. Louis area: A comparison between MISR and
1213 MODIS, *Remote sensing of Environment*, 107(1-2), 33-44,
1214 <https://doi.org/10.1016/j.rse.2006.05.022>, 2007.

1215 Liu, Y., Park, R. J., Jacob, D. J., Li, Q., Kilaru, V., and Sarnat, J. A.: Mapping annual mean ground-
1216 level PM_{2.5} concentrations using Multiangle Imaging Spectroradiometer aerosol optical
1217 thickness over the contiguous United States, *Journal of Geophysical Research:*
1218 *Atmospheres*, 109 (D22), <https://doi.org/10.1029/2004JD005025>, 2004.

1219 Liu, Y., Sarnat, J. A., Kilaru, V., Jacob, D. J., and Koutrakis, P.: Estimating ground-level PM_{2.5}
1220 in the eastern United States using satellite remote sensing, *Environmental science &*
1221 *technology*, 39(9), 3269-3278, doi: 10.1021/es049352m, 2005.

1222 Liou, Kuo-Nan.: An introduction to atmospheric radiation, Vol. 84. Academic press, 2002.

1223 Lynch P., and coauthors: An 11-year global gridded aerosol optical thickness reanalysis (v1.0) for

1224 atmospheric and climate sciences, Geosci. Model Dev., 9, 1489-1522, doi:10.5194/gmd-9-
1225 1489-2016, 2016.

1226 Malm, W.C. and Hand, J.L.: An examination of the physical and optical properties of aerosols
1227 collected in the IMPROVE program, Atmospheric Environment, 41(16), pp.3407-3427,
1228 <https://doi.org/10.1016/j.atmosenv.2006.12.012>, 2007.

1229 [Nessler, R., Weingartner, E., and Baltensperger, U. \(2005\). Effect of humidity on aerosol light](#)
1230 [absorption and its implications for extinction and the single scattering albedo illustrated for](#)
1231 [a site in the lower free troposphere, *Journal of Aerosol Science*, 36\(8\), 958-972.](#)

1232 Omar, A. H., Winker, D. M., Tackett, J. L., Giles, D. M., Kar, J., Liu, Z., Vaughan, M. A., Powell,
1233 K. A., and Trepte, C. R.: CALIOP and AERONET aerosol optical depth comparisons: One
1234 size fits none, J. Geophys. Res. Atmos., 118, 4748–4766, doi:10.1002/jgrd.50330, 2013.

1235 [Patashnick, H., Rupprecht, G., Ambs, J. L., and Meyer, M. B.: Development of a reference](#)
1236 [standard for particulate matter mass in ambient air, *Aerosol Science & Technology*, 34\(1\),](#)
1237 [42-45, 2001.](#)

1238 Reid, J. S., Eck, T. F., Christopher, S. A., Koppmann, R., Dubovik, O., Eleuterio, D. P., Holben,
1239 B. N., Reid, E. A., and Zhang, J.: A review of biomass burning emissions part III: intensive
1240 optical properties of biomass burning particles, Atmos. Chem. Phys., 5, 827-849,
1241 <https://doi.org/10.5194/acp-5-827-2005>, 2005.

1242 Reid, J. S. et al.: Skill of Operational Aerosol Forecast Models in Predicting Aerosol Events and
1243 Trends of the Eastern United States, A11B-001, AGU Fall meeting, San Francisco, 12-16
1244 Dec, 2016.

1245 Reid, J. S., Kuehn, R. E., Holz, R. E., Eloranta, E. W., Kaku, K. C., Kuang, S., ... and Atwood,

1246 S.A.: Ground-based High Spectral Resolution Lidar observation of aerosol vertical
1247 distribution in the summertime Southeast United States, *Journal of Geophysical Research:*
1248 *Atmospheres*, 122(5), 2970-3004, <https://doi.org/10.1002/2016JD025798>, 2017.

1249 Sessions, W. R., Reid, J. S., Benedetti, A., Colarco, P. R., da Silva, A., Lu, S., Sekiyama, T.,
1250 Tanaka, T. Y., Baldasano, J. M., Basart, S., Brooks, M. E., Eck, T. F., Iredell, M., Hansen,
1251 J. A., Jorba, O. C., Juang, H.-M. H., Lynch, P., Morcrette, J.-J., Moorthi, S., Mulcahy, J.,
1252 Pradhan, Y., Razinger, M., Sampson, C. B., Wang, J., and Westphal, D. L.: Development
1253 towards a global operational aerosol consensus: basic climatological characteristics of the
1254 International Cooperative for Aerosol Prediction Multi-Model Ensemble (ICAP-MME),
1255 *Atmos. Chem. Phys.*, 15, 335-362, <https://doi.org/10.5194/acp-15-335-2015>, 2015.

1256 Silva, R. A., West, J. J., Zhang, Y., Anenberg, S. C., Lamarque, J. F., Shindell, D. T., Collins,
1257 W.J., Dalsoren, S., Faluvegi, G., Folberth, G. & Horowitz, L. W.: Global premature
1258 mortality due to anthropogenic outdoor air pollution and the contribution of past climate
1259 change, *Environmental Research Letters*, 8(3), 034005, doi:10.1088/1748-
1260 9326/8/3/034005, 2013.

1261 [Spagnolo, G. S.: Automatic instrument for aerosol samples using the beta-particle attenuation,](#)
1262 [Journal of aerosol science, 20\(1\), 19-27, 1989.](#)

1263 Toth, T. D., Campbell, J. R., Reid, J. S., Tackett, J. L., Vaughan, M. A., Zhang, J., and Marquis,
1264 J. W.: Minimum aerosol layer detection sensitivities and their subsequent impacts on
1265 aerosol optical thickness retrievals in CALIPSO level 2 data products, *Atmos. Meas. Tech.*,
1266 11, 499-514, <https://doi.org/10.5194/amt-11-499-2018>, 2018.

1267 Toth, T. D., Zhang, J., Campbell, J. R., Hyer, E. J., Reid, J. S., Shi, Y., and Westphal, D. L.: Impact

1268 of data quality and surface-to-column representativeness on the PM_{2.5} / satellite AOD
1269 relationship for the contiguous United States, *Atmos. Chem. Phys.*, 14, 6049-6062,
1270 <https://doi.org/10.5194/acp-14-6049-2014>, 2014.

1271 Toth, T. D., Zhang, J., Campbell, J. R., Reid, J. S., Shi, Y., Johnson, R. S., Smirnov, A., Vaughan,
1272 M.A. and Winker, D. M.: Investigating enhanced Aqua MODIS aerosol optical depth
1273 retrievals over the mid-to-high latitude Southern Oceans through intercomparison with co-
1274 located CALIOP, MAN, and AERONET data sets, *Journal of Geophysical Research:*
1275 *Atmospheres*, 118(10), 4700-4714, <https://doi.org/10.1002/jgrd.50311>, 2013.

1276 Toth, T. D., Zhang, J., Campbell, J. R., Reid, J. S., and Vaughan, M. A.: Temporal variability of
1277 aerosol optical thickness vertical distribution observed from CALIOP, *Journal of*
1278 *Geophysical Research: Atmospheres*, 121(15), 9117-9139,
1279 <https://doi.org/10.1002/2015JD024668>, 2016.

1280 Val Martin, M., Heald, C. L., Ford, B., Prenni, A. J., and Wiedinmyer, C.: A decadal satellite
1281 analysis of the origins and impacts of smoke in Colorado, *Atmos. Chem. Phys.*, 13, 7429-
1282 7439, <https://doi.org/10.5194/acp-13-7429-2013>, 2013.

1283 Van Donkelaar, A., Martin, R. V., Brauer, M., Kahn, R., Levy, R., Verduzco, C., and Villeneuve,
1284 P. J.: Global Estimates of Ambient Fine Particulate Matter Concentrations from Satellite
1285 Based Aerosol Optical Depth: Development and Application, *Environ. Health Perspect.*,
1286 118(6): 847–855, <https://dx.doi.org/10.1289%2Fehp.0901623>, 2010.

1287 Van Donkelaar, A., Martin, R. V., Spurr, R. J., and Burnett, R. T.: High-resolution satellite-derived
1288 PM_{2.5} from optimal estimation and geographically weighted regression over North
1289 America, *Environmental science & technology*, 49.17 (2015): 10482-10491,
1290 doi: 10.1021/acs.est.5b02076, 2015.

1291 Waggoner, A. P., and Weiss, R. E.: Comparison of fine particle mass concentration and light
1292 scattering extinction in ambient aerosol, *Atmospheric Environment* (1967), 14(5), 623-
1293 626, [https://doi.org/10.1016/0004-6981\(80\)90098-0](https://doi.org/10.1016/0004-6981(80)90098-0), 1980.

1294 Wang, J., and Christopher, S. A.: Intercomparison between satellite-derived aerosol optical
1295 thickness and PM_{2.5} mass: implications for air quality studies, *Geophysical research*
1296 *letters*, 30(21), <https://doi.org/10.1029/2003GL018174>, 2003.

1297 Winker, D. M., Hunt, W. H., and McGill, M. J.: Initial performance assessment of CALIOP,
1298 *Geophysical Research Letters*, 34(19), <https://doi.org/10.1029/2007GL030135>, 2007.

1299 Winker, D. M., Pelon, J., Coakley Jr, J. A., Ackerman, S. A., Charlson, R. J., Colarco, P. R., ...
1300 and Kubar, T. L.: The CALIPSO mission: A global 3D view of aerosols and clouds,
1301 *Bulletin of the American Meteorological Society*, 91(9), 1211-1230,
1302 <https://doi.org/10.1175/2010BAMS3009.1>, 2010.

1303 Winker, D. M., Vaughan, M. A., Omar, A., Hu, Y., Powell, K. A., Liu, Z., Hunt, W. H., and Young,
1304 S. A.: Overview of the CALIPSO Mission and CALIOP Data Processing Algorithms, *J.*
1305 *Atmos. Oceanic Technol.*, 26, 2310–2323, <https://doi.org/10.1175/2009JTECHA1281.1>,
1306 2009.

1307 Young, S. A., Vaughan, M. A., Kuehn, R. E., and Winker, D. M.: The retrieval of profiles of
1308 particulate extinction from Cloud–Aerosol Lidar and Infrared Pathfinder Satellite
1309 Observations (CALIPSO) data: Uncertainty and error sensitivity analyses, *Journal of*
1310 *Atmospheric and Oceanic Technology*, 30(3), 395-428,
1311 <https://doi.org/10.1175/2009JTECHA1281.1>, 2013.

1312 Zhang, J., Campbell, J.R., Hyer, E. J., Reid, J.S., Westphal, D. L., and Johnson, R. S.: Evaluating

1313 the impact of multisensor data assimilation on a global aerosol particle transport model, J.
1314 Geophys. Res. Atmos., 119, 4674–4689, doi:10.1002/2013JD020975, 2014.

1315 Zhang, J. and Reid, J.S.: An analysis of clear sky and contextual biases using an operational over
1316 ocean MODIS aerosol product, Geophysical Research Letters, 36, L15824,
1317 doi:10.1029/2009GL038723, 2009.

1318

1319

1320

1321

1322

1323

1324

1325

1326

1327

1328

1329

1330

1331

1332

1333

1334

1335

1336

1337

1338

1339

1340

1341

1342

1343

1344

1345

1346

1347

1348

1349

1350

1351

1352 **Figure and Table Captions**

1353

1354 Figure 1. For 2008-2009, scatterplot of mean PM_{2.5} concentration from ground-based U.S. EPA
1355 stations and mean column AOD (550 nm) from collocated Collection 6 (C6) Aqua MODIS
1356 observations. The red line represents the Deming regression fit.

1357

1358 Figure 2. For 2008-2009 over the CONUS, (a) mean PM_{2.5} concentration ($\mu\text{g m}^{-3}$) for those U.S.
1359 EPA stations with reported daily measurements, and (c) $1^\circ \times 1^\circ$ average CALIOP-derived PM_{2.5}
1360 concentrations for the 100–1000 m AGL atmospheric layer, using Equation 3, for combined
1361 daytime and nighttime conditions. Also shown are the pairwise PM_{2.5} concentrations from (b)
1362 EPA daily measurements and (d) those derived from CALIOP (day and night combined), both
1363 averaged for each EPA station for the 2008-2009 period. For all four plots, values greater than 20
1364 $\mu\text{g m}^{-3}$ are colored red.

1365

1366 Figure 3. For 2008-2009 over the CONUS, $1^\circ \times 1^\circ$ average CALIOP extinction, relative to the
1367 number of cloud-free 5 km CALIOP profiles in each $1^\circ \times 1^\circ$ bin, for the 100 – 1000 m AGL
1368 atmospheric layer, for (a) daytime and (b) nighttime measurements. Also shown are the
1369 corresponding CALIOP-derived PM_{2.5} concentrations, using Equation 3 for (c) daytime and (d)
1370 nighttime conditions. Values greater than 0.2 km^{-1} and $20 \mu\text{g m}^{-3}$ for (a, b) and (c, d), respectively,
1371 are colored red. Scatterplots of mean PM_{2.5} concentration from ground-based U.S. EPA stations
1372 and those derived from collocated near-surface CALIOP observations are shown in the bottom
1373 row, using (e) daytime and (f) nighttime CALIOP data. The red lines represent the Deming
1374 regression fits.

1375 Figure 4. Scatterplot of mean $PM_{2.5}$ concentration from ground-based U.S. EPA stations and those
1376 derived from collocated near-surface CALIOP observations using combined daytime and
1377 nighttime CALIOP data. The red line represents the Deming regression fit.

1378

1379 Figure 5. Root-mean-square errors of CALIOP-derived $PM_{2.5}$ against EPA $PM_{2.5}$ as a function of
1380 CALIOP-derived $PM_{2.5}$, using both daytime (in red) and nighttime (in blue) CALIOP observations.
1381 The five bins are equally sampled based upon a cumulative histogram analysis, and each point
1382 from left to right represents the RMSE and mean $PM_{2.5}$ concentration derived from CALIOP for
1383 0-20%, 20-40%, 40-60%, 60-80%, and 80-100% cumulative frequencies.

1384

1385 Figure 6. Two-year (2008-2009) histograms of mean $PM_{2.5}$ concentrations from the U.S. EPA (in
1386 black) and those derived from aerosol extinction using nighttime (in blue) and daytime (in red)
1387 CALIOP data. The U.S. EPA data shown are not collocated, while those derived using CALIOP
1388 are spatially (but not temporally) collocated, with EPA station observations.


1389

1390 Figure 7. Two-year (2008-2009) histograms of mean $PM_{2.5}$ concentrations from the U.S. EPA and
1391 those derived from spatially and temporally collocated aerosol extinction using (a) daytime and
1392 (b) nighttime CALIOP data.

1393

1394 Figure 8. For 2008-2009, scatterplots of mean $PM_{2.5}$ concentration from ground-based U.S. EPA
1395 stations and mean column AOD from collocated CALIOP observations, using (a) daytime and (b)
1396 nighttime CALIOP data. The red lines represent the Deming regression fits.

1397

Deleted: Root-mean-square errors of CALIOP-derived $PM_{2.5}$ against EPA $PM_{2.5}$ as a function of CALIOP-derived $PM_{2.5}$ (filled circles), and corresponding number of data samples per bin (X symbols), using both daytime (in red) and nighttime (in blue) CALIOP observations. 

Deleted:

1404 Figure 9. For 2008-2009, scatterplots of mean PM_{2.5} concentration from ground-based U.S. EPA
1405 stations and those derived from collocated all-sky (including cloud-free and cloudy profiles) near-
1406 surface CALIOP observations, using (a) daytime and (b) nighttime CALIOP data. The red lines
1407 represent the Deming regression fits.
1408

1409 Figure 10. For 2008-2009 over the CONUS, scatterplot of distance (km) between any two U.S.
1410 EPA stations and the corresponding spatial correlation of PM_{2.5} concentration between each pair
1411 of stations. The black curve represents the exponential fit to the data for the entire CONUS, and
1412 the red and blue dashed lines represent 10 km bin averages for the Western and Eastern CONUS,
1413 respectively.
1414

1415 Table 1. The parameters, and corresponding values, used to quality assure the CALIOP aerosol
1416 extinction profile.
1417

1418 Table 2. Statistical summary of a sensitivity analysis varying the height of the surface layer,
1419 including R², slope from Deming regression, mean bias (CALIOP - EPA) of PM_{2.5} in µg m⁻³, and
1420 percent error change in derived PM_{2.5}, defined as: ((mean new PM_{2.5} – mean original PM_{2.5})/mean
1421 original PM_{2.5})*100. The row in bold represents the results shown in the remainder of the paper.
1422

Deleted: , slope

1423 Table 3. Statistical summary of a sensitivity analysis varying the PM_{2.5} to PM₁₀ ratio used,
1424 including slope from Deming regression, mean bias (CALIOP - EPA) of PM_{2.5} in µg m⁻³, and
1425 percent error change in derived PM_{2.5}, defined as: ((mean new PM_{2.5} – mean original PM_{2.5})/mean
1426 original PM_{2.5})*100. The row in bold represents the results shown in the remainder of the paper.

Deleted: slope,

1429

1430 Table 4. Statistical summary of a sensitivity analysis varying the aerosol type assumed in the
1431 derivation of PM_{2.5}, including R², slope from Deming regression, mean bias (CALIOP - EPA) of
1432 PM_{2.5} in µg m⁻³, and percent error change in derived PM_{2.5}, defined as: ((mean new PM_{2.5} – mean
1433 original PM_{2.5})/mean original PM_{2.5})*100. The row in bold represents the results shown in the
1434 remainder of the paper.

1435

1436 Appendix Figure 1. For 2008-2009 over the CONUS, for each 1° x 1° grid box, the number of
1437 days and CALIOP Level 2 5 km aerosol profiles used in the creation of the maps in Fig. 3 for (a,
1438 c) daytime and (b, d) nighttime measurements. Values greater than 400 profiles for (c, d) are
1439 colored red.

1440

1441

1442

1443

1444

1445

1446

1447

1448

1449

1450

1451

1452

1453

1454

1455

1456

1457

Deleted: , slope

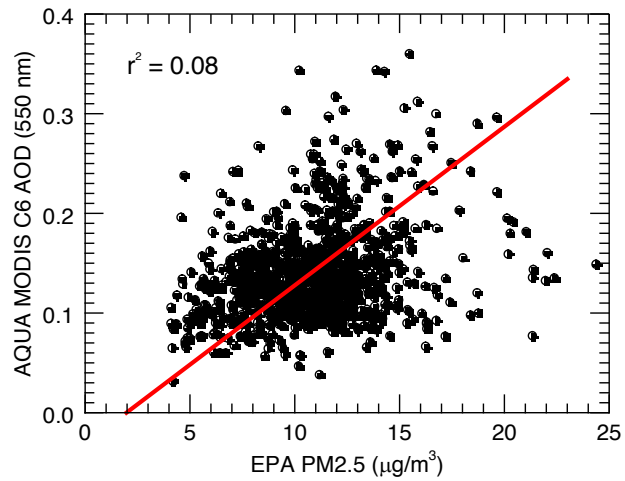


Figure 1. For 2008-2009, scatterplot of mean PM_{2.5} concentration from ground-based U.S. EPA stations and mean column AOD (550 nm) from collocated Collection 6 (C6) Aqua MODIS observations. The red line represents the Deming regression fit.

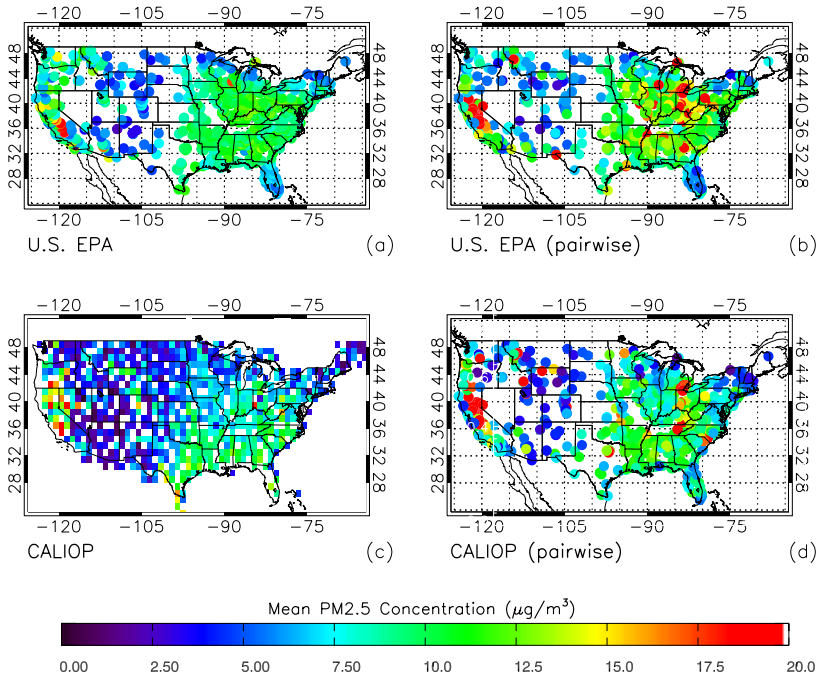


Figure 2. For 2008-2009 over the CONUS, (a) mean PM_{2.5} concentration (µg m⁻³) for those U.S. EPA stations with reported daily measurements, and (c) 1° x 1° average CALIOP-derived PM_{2.5} concentrations for the 100–1000 m AGL atmospheric layer, using Equation 3, for combined daytime and nighttime conditions. Also shown are the pairwise PM_{2.5} concentrations from (b) EPA daily measurements and (d) those derived from CALIOP (day and night combined), both averaged for each EPA station for the 2008-2009 period. For all four plots, values greater than 20 µg m⁻³ are colored red.

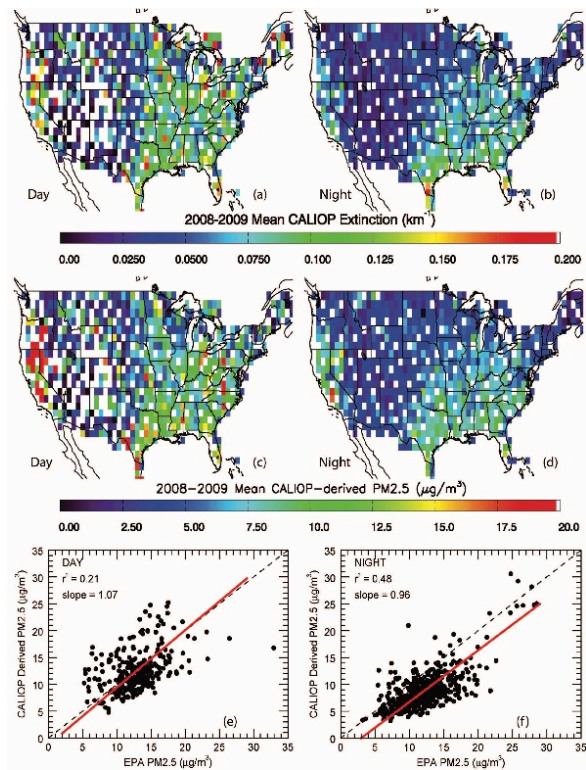


Figure 3. For 2008-2009 over the CONUS, $1^\circ \times 1^\circ$ average CALIOP extinction, relative to the number of cloud-free L2_05kmAPro profiles in each $1^\circ \times 1^\circ$ bin, for the 100 – 1000 m AGL atmospheric layer, for (a) daytime and (b) nighttime measurements. Also shown are the corresponding CALIOP-derived $\text{PM}_{2.5}$ concentrations, using Equation 3 for (c) daytime and (d) nighttime conditions. Values greater than 0.2 km^{-1} and $20 \mu\text{g m}^{-3}$ for (a, b) and (c, d), respectively, are colored red. Scatterplots of mean $\text{PM}_{2.5}$ concentration from ground-based U.S. EPA stations and those derived from collocated near-surface CALIOP observations are shown in the bottom row, using (e) daytime and (f) nighttime CALIOP data. The red lines represent the Deming regression fits.

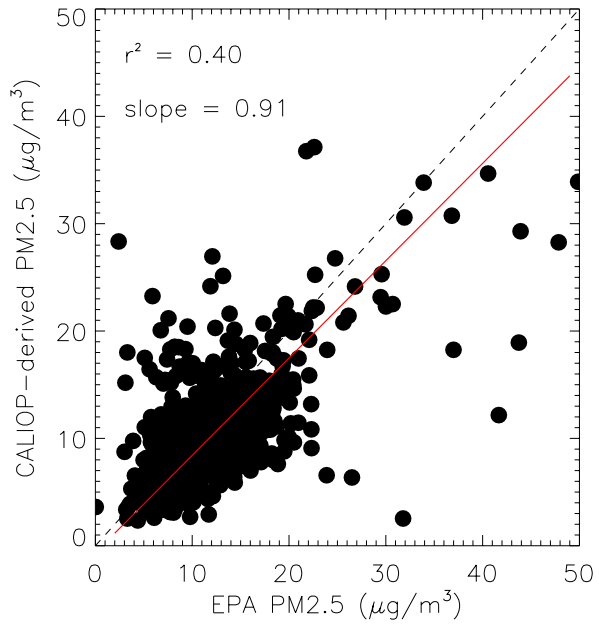


Figure 4. Scatterplot of mean PM_{2.5} concentration from ground-based U.S. EPA stations and those derived from collocated near-surface CALIOP observations using combined daytime and nighttime CALIOP data. The red line represents the Deming regression fit.

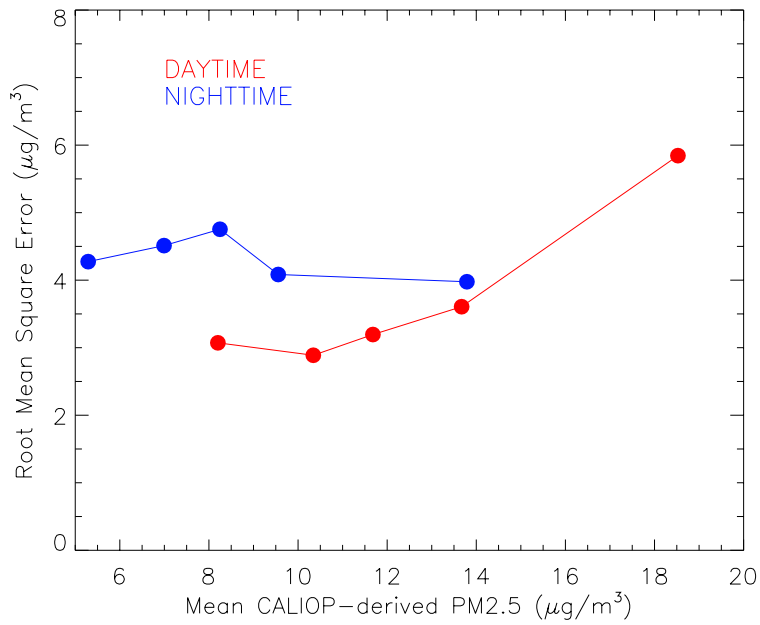


Figure 5. Root-mean-square errors of CALIOP-derived PM_{2.5} against EPA PM_{2.5} as a function of CALIOP-derived PM_{2.5}, using both daytime (in red) and nighttime (in blue) CALIOP observations. The five bins are equally sampled based upon a cumulative histogram analysis, and each point from left to right represents the RMSE and mean PM_{2.5} concentration derived from CALIOP for 0-20%, 20-40%, 40-60%, 60-80%, and 80-100% cumulative frequencies.

1465
 1466
 1467
 1468
 1469
 1470
 1471
 1472
 1473
 1474

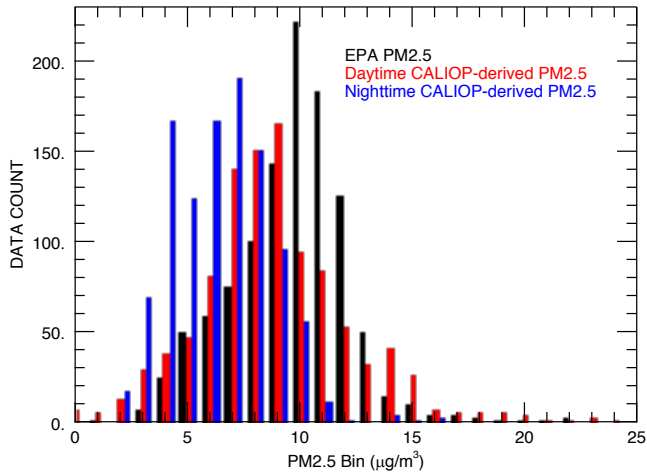


Figure 6. Two-year (2008-2009) histograms of mean PM_{2.5} concentrations from the U.S. EPA (in black) and those derived from aerosol extinction using nighttime (in blue) and daytime (in red) CALIOP data. The U.S. EPA data shown are not collocated, while those derived using CALIOP are spatially (but not temporally) collocated, with EPA station observations.

1475
 1476
 1477
 1478
 1479
 1480
 1481

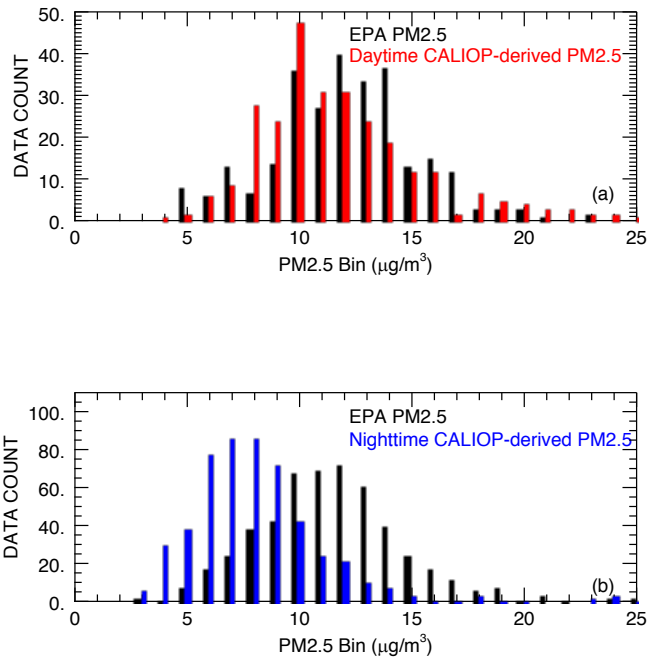


Figure 7. Two-year (2008-2009) histograms of mean PM_{2.5} concentrations from the U.S. EPA and those derived from spatially and temporally collocated aerosol extinction using (a) daytime and (b) nighttime CALIOP data.

1482
 1483
 1484
 1485
 1486
 1487
 1488
 1489
 1490
 1491

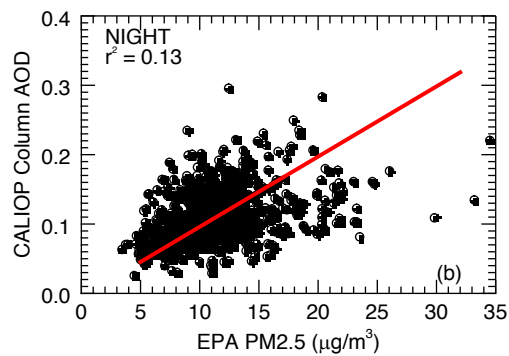
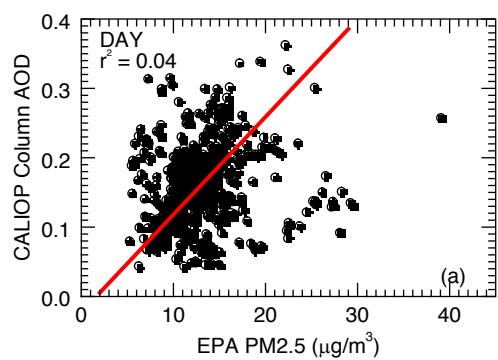


Figure 8. For 2008-2009, scatterplots of mean PM_{2.5} concentration from ground-based U.S. EPA stations and mean column AOD from collocated CALIOP observations, using (a) daytime and (b) nighttime CALIOP data. The red lines represent the Deming regression fits.

1492
1493

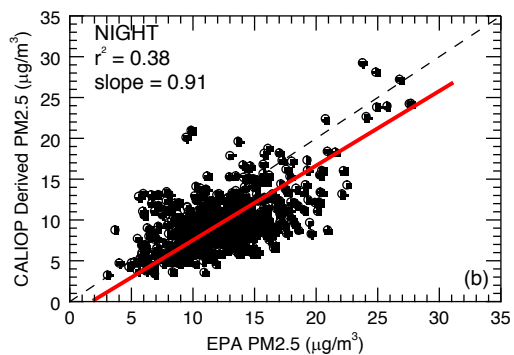
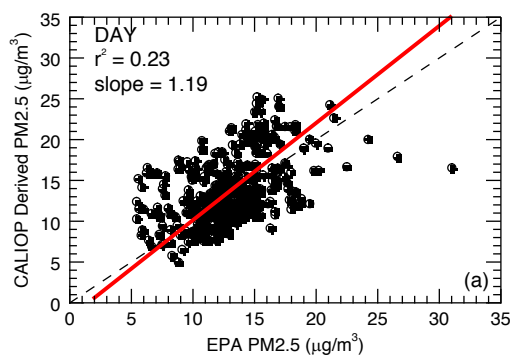


Figure 9. For 2008-2009, scatterplots of mean PM_{2.5} concentration from ground-based U.S. EPA stations and those derived from collocated all-sky (including cloud-free and cloudy profiles) near-surface CALIOP observations, using (a) daytime and (b) nighttime CALIOP data. The red lines represent the Deming regression fits.

1494
 1495
 1496
 1497

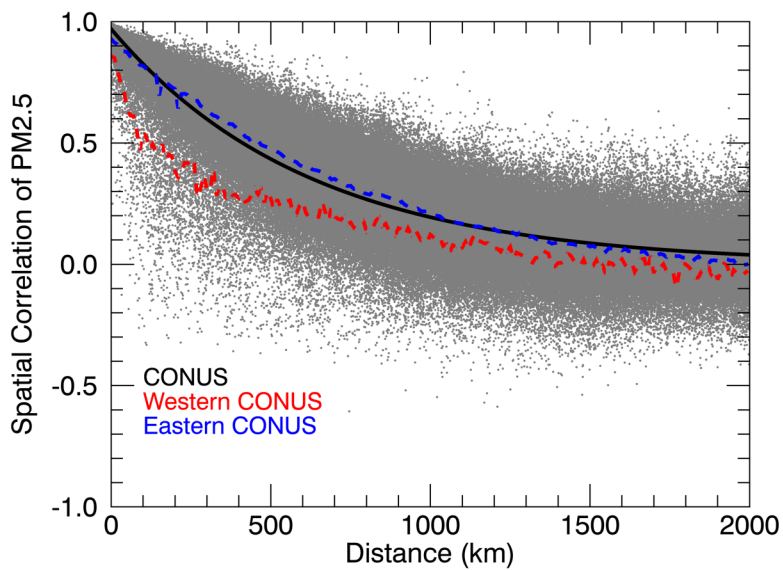


Figure 10. For 2008-2009 over the CONUS, scatterplot of distance (km) between any two U.S. EPA stations and the corresponding spatial correlation of PM_{2.5} concentration between each pair of stations. The black curve represents the exponential fit to the data for the entire CONUS, and the red and blue dashed lines represent 10 km bin averages for the Western and Eastern CONUS, respectively.

1498
1499
1500
1501

1502
1503
1504
1505
1506

Tables

Parameter	Values
Integrated_Attenuated_Backscatter_532	$\leq 0.01 \text{ sr}^{-1}$
Extinction_Coefficient_532	≥ 0 and $\leq 1.25 \text{ km}^{-1}$
Extinction_QC_532	= 0, 1, 2, 16, or 18
CAD_Score	≥ -100 and ≤ -20
Extinction_Coefficient_Uncertainty_532	$\leq 10 \text{ km}^{-1}$
Atmospheric_Volume_Description (Bits 1-3)	= 3
Atmospheric_Volume_Description (Bits 10-12)	$\neq 0$

Table 1. The parameters, and corresponding values, used to quality assure the CALIOP aerosol extinction profile.

1507
1508
1509
1510
1511
1512
1513
1514
1515
1516

1517
1518
1519

Surface Layer (m)	Analysis (Day/Night)			
	R ²	Deming Slope	Mean Bias (CALIOP - EPA; $\mu\text{g m}^{-3}$)	Error Change (%)
0-100	0.27/0.41	1.32/0.60	-2.67/-9.06	-13.71/-61.94
0-200	0.33/0.53	1.34/1.04	-0.52/-5.68	3.79/-23.58
0-300	0.35/0.54	1.32/1.11	-0.09/-4.70	7.24/-12.15
0-400	0.38/0.57	1.30/1.13	-0.13/-4.25	6.92/-6.46
0-500	0.35/0.52	1.26/1.06	-0.21/-4.04	5.70/-4.39
0-600	0.40/0.53	1.19/1.04	-0.46/-3.91	3.72/-2.15
0-700	0.44/0.46	1.20/0.98	-0.41/-3.89	2.73/-2.88
0-800	0.35/0.50	1.06/0.94	-0.59/-3.76	-0.77/-2.04
0-900	0.17/0.49	1.04/0.91	-0.74/-3.74	-3.91/-2.25
0-1000	0.13/0.48	0.98/0.89	-1.08/-3.74	-7.48/-2.57
100-500	0.34/0.44	1.23/1.00	0.54/-3.40	14.21/-0.84
100-1000	0.21/0.48	1.07/0.96	-0.39/-3.34	

Table 2. Statistical summary of a sensitivity analysis varying the height of the surface layer, including R², slope from Deming regression, mean bias (CALIOP - EPA) of PM_{2.5} in $\mu\text{g m}^{-3}$, and percent error change in derived PM_{2.5}, defined as: $((\text{mean new PM}_{2.5} - \text{mean original PM}_{2.5})/\text{mean original PM}_{2.5}) * 100$. The row in bold represents the results shown in the remainder of the paper.

1520
1521
1522
1523
1524
1525
1526
1527
1528
1529
1530
1531

1532
1533
1534

PM _{2.5} /PM ₁₀ Ratio	Analysis (Day/Night)		
	Deming Slope	Mean Bias (CALIOP - EPA; $\mu\text{g m}^{-3}$)	% Error Change
Low ratio (-1 STDEV) = 0.24	0.43/0.38	-7.81/-8.61	-60.00%/-60.00%
High ratio (+1 STDEV) = 0.88	1.57/1.41	5.39/0.77	46.67%/46.67%
0.6	1.07/0.96	-0.39/-3.34	

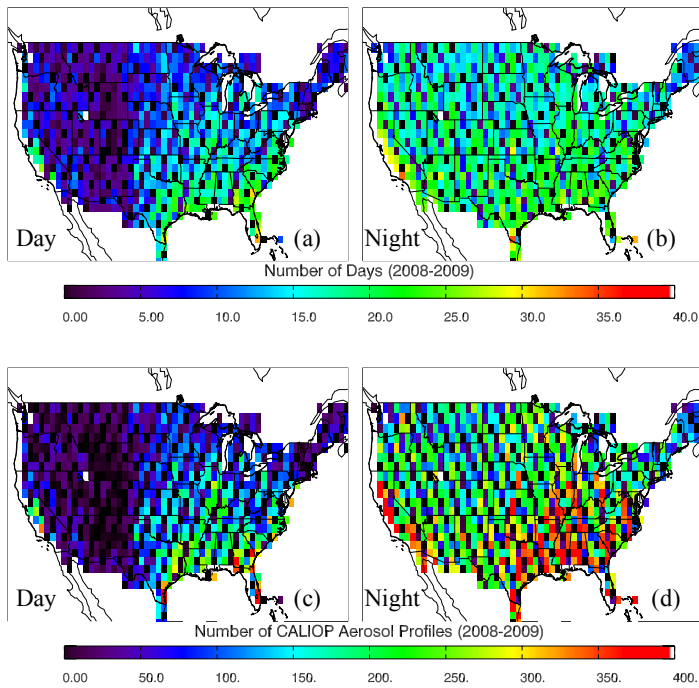
Table 3. Statistical summary of a sensitivity analysis varying the PM_{2.5} to PM₁₀ ratio used, including slope from Deming regression, mean bias (CALIOP - EPA) of PM_{2.5} in $\mu\text{g m}^{-3}$, and percent error change in derived PM_{2.5}, defined as: ((mean new PM_{2.5} – mean original PM_{2.5})/mean original PM_{2.5})*100. The row in bold represents the results shown in the remainder of the paper.

1535
1536
1537
1538
1539
1540
1541
1542

Analysis (Day/Night)							
Aerosol Type			R ²	Deming Slope	Mean Bias (CALIOP - EPA; $\mu\text{g m}^{-3}$)	% Error Change	
	a _{scat}	a _{abs}	Γ				
Smoke	5.26	0.26	0.18	0.10/0.44	0.86/0.78	-1.81/-4.26	-11.53/-10.54
Sea salt	1.42	0.01	0.46	0.18/0.48	2.92/2.64	22.42/12.93	184.12/184.99
Dust	0.52	0.08	0.00	0.05/0.39	9.01/8.18	102.04/70.82	826.94/843.33
Sulfate	3.4	0.37	0.63	0.21/0.48	1.07/0.96	-0.39/-3.34	

Table 4. Statistical summary of a sensitivity analysis varying the aerosol type assumed in the derivation of $\text{PM}_{2.5}$, including R^2 , slope from Deming regression, mean bias (CALIOP - EPA) of $\text{PM}_{2.5}$ in $\mu\text{g m}^{-3}$, and percent error change in derived $\text{PM}_{2.5}$, defined as: $((\text{mean new } \text{PM}_{2.5} - \text{mean original } \text{PM}_{2.5}) / \text{mean original } \text{PM}_{2.5}) * 100$. The row in bold represents the results shown in the remainder of the paper.

1543
1544
1545
1546
1547
1548



Appendix Figure 1. For 2008-2009 over the CONUS, for each 1° x 1° grid box, the number of days and CALIOP Level 2 5 km aerosol profiles used in the creation of the maps in Fig. 3 for (a, c) daytime and (b, d) nighttime measurements. Values greater than 400 profiles for (c, d) are colored red.

1549
1550
1551